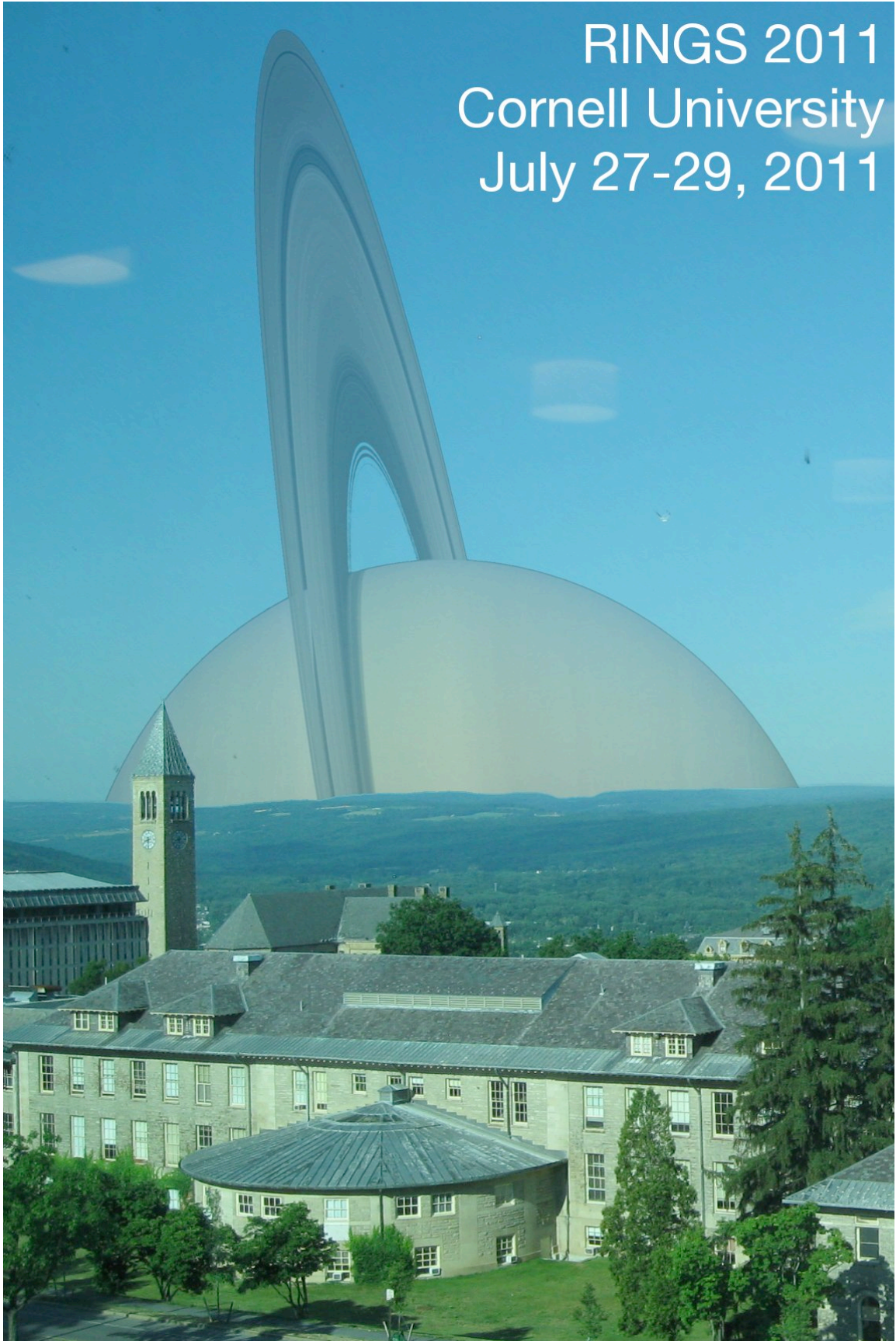


RINGS 2011  
Cornell University  
July 27-29, 2011



# Block Schedule

---

	Wednesday 7/27	Thursday 7/28	Friday 7/29
8:30	Introduction		Ring Objects
8:40	Dense Ring Structure	Ring Composition	
9:00			
9:20			
9:40			
10:00			
10:20	Dense Ring Structure (continued)	Ring Particle Properties	F ring
10:40			
11:00			
11:20			
11:40			
12:00			
12:20			
12:40	Lunch	Lunch	Lunch
13:00			
13:20			
13:40			
14:00		Ring Particle Sizes	Ring Origins
14:20	Dusty Rings		
14:40			
15:00			
15:20		OPUS	
15:40	Dusty Rings and Ring Environments	Intro to Posters	Ring Evolution
16:00		Poster Session	
16:20			
16:40			
17:00			Discussion
17:20	Discussion		
17:40			
18:00			
18:30	Dinner on Campus	BBQ at Treman Park	Open
19:00			
19:30			

## Wednesday Morning, July 27

---

- 8:30-8:40    **Welcome, Introduction**
- 8:40-9:00    *Revisiting the Self-Gravity Wakes Granola Bar Model:  
More Data, More Parameters*  
**J. E. Colwell**, R. G. Jerousek, J. H. Cooney
- 9:00-9:20    *Self-Gravity Wakes and the Viscosity of Dense Planetary Rings*  
**G. R. Stewart**
- 9:20-9:40    *B Ring Gray Ghosts in Cassini UVIS Occultations*  
**M. Sremčević** L.W. Esposito, J.E. Colwell, N. Albers
- 9:40-10:00    *Simulating the B ring*  
**M. Lewis**
- 10:00-10:20    **Break**
- 10:20-10:40    *Noncircular Features in Saturn's Rings: I. The Cassini Division*  
**R. G. French**, P. D. Nicholson, J. Colwell, E. A. Marouf, N. J. Rappaport,  
M. Hedman, K. Lonergan, C. McGhee-French, and T. Sepersky
- 10:40-11:00    *Noncircular Features in Saturn's Rings: II. The C ring*  
**P. D. Nicholson**, R. G. French, M. M. Hedman, E. A. Marouf,  
J. E. Colwell, N. Rappaport, T. L. Sepersky and K. R. Lonergan
- 11:00-11:20    *Analysis of Saturn's Huygens Ringlet using Cassini ISS images*  
**J. N. Spitale**, C. C. Porco, J. M. Hahn
- 11:20-11:40    *Global N-body Integrations of Planetary Rings*  
**J. M. Hahn**, J.N. Spitale
- 11:40-12:10    *The Core of Ring F and New Corrugation Structure in Ring C*  
**E. Marouf** R. Franch, N. Rappaport, K. Wong,  
C. McGhee-French, A. Anabtawi
- 12:10-14:00    **Lunch**

## Wednesday Afternoon, July 27

---

- 14:00-14:20 *The Rings of Uranus: Shepherded, or Not?*  
**M.R. Showalter**
- 14:20-14:40 *The Activity of Spokes in Saturn's B Ring*  
**C. Mitchell**, C.C. Porco, L. Dones, J.N. Spitale
- 14:40-15:00 *The Structure of Saturn's E ring as seen by Cassini CDA*  
**S. Kempf**, R. Srama, G. Moragas-Klostermeyer, F. Postberg,  
J. Schmidt, F. Spahn
- 15:00-15:20 *The E ring Re-imaged and Re-imagined*  
**J.A. Burns**, M.M. Hedman, D.P. Hamilton, M.R. Showalter
- 15:20-15:40 **Break**
- 15:40-16:00 *Circumplanetary Dust in Multipolar Magnetic Fields*  
**D. Jontof-Hutter**, D.P. Hamilton
- 16:00-16:20 *Evolution of Circumplanetary Dust Orbits  
at High Eccentricity due to Resonant Charge Variations*  
**L. Schaffer**
- 16:20-16:40 *Chaotic Dust Orbits at Uranus may Explain  
Hemispherical Color Asymmetries Common to its Regular Satellites*  
**D. Tamayo**, J.A. Burns, D.P. Hamilton, P.D. Nicholson
- 16:40-17:00 *Plasma Variations in Saturn's Inner Magnetosphere  
from the Main Rings to Enceladus*  
**M.K. Elrod** W.L. Tseng, R.E. Johnson
- 17:00-18:00 **Discussion**

## Thursday Morning, July 28

---

- 8:40-9:00     *Scattering Properties of Saturn's Rings  
in the Far Ultraviolet from Cassini UVIS Spectra*  
**E.T. Bradley**, J.E. Colwell, L.W. Esposito
- 9:00-9:20     *The Composition of Saturn's Rings from Cassini VIMS*  
**R.N. Clark**, J. Cuzzi, G. Filacchione, D. P. Cruikshank, P. D. Nicholson,  
M. M. Hedman, R. H. Brown, B. J. Buratti, K. H. Baines, R. M. Nelson
- 9:20-9:40     *Saturn's Rings: What's the Red Stuff and How Much is There?*  
**J. Cuzzi**, S. Vahidinia
- 9:40-10:00    *Interactions of Saturn's Moons with its Ring Rystem*  
**B.J. Buratti**
- 10:00-10:20   **Break**
- 10:20-10:40   *Using Spectra to Probe the Densest Parts of Saturns Rings*  
**M.M. Hedman**, P.D. Nicholson
- 10:40-11:00   *Mapping Ring Shadow Cooling and Thermal Inertia with Cassini CIRS*  
**S.M. Brooks**, L.J. Spilker, R. Morishima
- 11:00-11:20   *On the Nature of the Scattering in Thermal Data of the Saturn's Rings*  
**E. Deau**, L.J. Spiker, R. Morishima
- 11:20-11:40   *Modeling Thermal Transport and Emission of Particle Ensembles*  
**S. Piorz**
- 11:40-12:00   *Modeling Saturn Ring Temperature Changes at Equinox*  
**L. Spilker**, C. Ferrari, R. Morishima
- 12:00-13:40   **Lunch**

## Thursday Afternoon, July 28

---

- 13:40-14:00 *Particle Size Variations in Saturn's Rings from Occultation Statistics*  
J.E. Colwell, **J.C. Cooney**, L.W. Esposito
- 14:00-14:20 *Measuring Centimeter-Sized Particles in the Saturnian Rings  
by Diffraction of Starlight*  
**R.A. Harbison**, P.D. Nicholson
- 14:20-14:40 *Kinetics of Aggregation and Fragmentation - Size Distribution of Rings*  
**F. Spahn**, E.V. Neto, A.H. Gulimares, N.V. Brilliantov, A.N. Gorban
- 14:40-15:00 *A Kinetic Fragmentation and Coagulation Model  
for the Distribution of Particle Sizes in Saturn's Rings*  
N.V. Brilliantov, P. Krapivsky, H. Hayakawa, A. Bodrova, F. Spahn,  
**J. Schmidt**
- 15:00-15:20 *OPUS: A Tool to Obtain Ring Data from the Planetary Data System*  
**M.K. Gordon**
- 15:20-15:40 **Break**

## Thursday Posters, July 28

---

*The B Ring Edge: Impressions from Voyager ISS and Cassini UVIS*

**N. Albers**, M. Sremcevic, L.W. Esposito

*A Catalog of Features in Saturn's Rings from Cassini Occultation Observations*

**K.R. Lonergan**, T.L. Sepersky, R.G. French

*The Geometry of Saturn's Rings from Cassini Occultation Observations*

**T.L. Sepersky**, K.R. Lonergan, R.G. French

*Effects of Inclination and Longitude of the Ascending Node  
of Gap Moons on Structure of Moon Wakes*

**A. Ducey**, M. Lewis

*N-Body Simulations of Silicate Hiding In Saturn's Dense Rings*

**G. Jones**, M. Lewis

*Fine-Scale Self-Gravity Density Wave Structure of Saturn's Main Rings*

**E. Griv**, M. Gedalin

*Velocity-Anisotropy-Driven Bending Instability in the Main Jovian Ring  
and Saturn's Faint D and C Rings*

**E. Griv**

*Cassini UVIS Observations of Saturn's Faint, Narrow Ringlets*

**B. Bolin**, J.E. Colwell

*Dust-Plasma Interaction in the Rings of Saturn*

**M. Holmberg** J.-E. Wahlund, M. Morooka, S. Sakai

*How Simulations Reveal Features in the Rings of Saturn*

**E. Khalisi**

## Thursday Posters, July 28

---

*Thermal Inertia of Icy Particles of Saturn's Rings Inferred From Cassini CIRS*

**R. Morishima**, L. Spilker, K. Ohtsuki

*Formation of a Propeller Structure by a Moonlet in a Dense Planetary Ring*

**S. Michikoshi**

*Viscosity in Planetary Rings with Spinning Self-Gravitating Particles*

*Obtained by N-body Simulation*

**Y. Yasui**, K. Ohtsuki, H. Daisaka

*Constraining Size Distribution in the F Ring*

**T. Becker**, J.E. Colwell

*Dynamical Stability of Saturn's F ring*

**A.D. Whizin**, J.E. Colwell, J.N. Cuzzi

*Capture of Irregular Satellites via Binary Planetesimal Exchange*

*in Migrating Planetary Systems*

**Imran Hassan**, Alex Moore, Alice Quillen

*Eclipses by Circumsecondary and Circumplanetary Disks and a Candidate Long and Deep Eclipse of a Pre-main Sequence Star in Sco-Cen*

**Eric Mamajek**, Alice Quillen, Mark Pecaut, Fred Moolekamp,  
Erin Scott, Matt Kenworthy Andrew Collier Cameron, Neil Parley

*Stability of Multiple Planet or Satellite Systems*

**Alice Quillen**

## Friday Morning, July 29

---

- 8:40-9:00 *Small Propeller Signatures in the C Ring and Cassini Division*  
**K. Baillie**, J.E. Colwell, L.W. Esposito
- 9:00-9:20 *The Propeller and the Frog*  
**M. Pan**
- 9:20-9:40 *Strands and Clumps in Saturn's F ring*  
**C.D. Murray**, N. Cooper, G.A. Williams, M.W. Evans, T. Wong
- 9:40-10:00 *The Structures of the Saturnian F Ring: Observations and Modeling*  
**N. Albers**, M. Sremcevic, L.W. Esposito
- 10:00-10:20 **Break**
- 10:20-10:40 *The Brightening of Saturn's F Ring*  
**R.S. French**, M.R. Showalter, R. Sfair, C. Argelles,  
M. Pajuelo, P. Becerra, M.M. Hedman, P.D. Nicholson
- 10:40-11:00 *The Mass of Transient Clumps in Saturn's F Ring*  
**B. Meinke**, L.W. Esposito, M. Sremcevic
- 11:00-11:20 *The Height of Saturn's F Ring in VIMS and ISS Observations of a Cassini Ring-Plane Crossing*  
**B.R. Scharringhausen** M.S. Crumrine, S.R. Storck-Post,  
M.E. Rehnberg, S.A. Sans, S.M. Wolfe
- 11:20-11:40 *Saturn's F ring Grains: Aggregates Made of Crystalline Water Ice*  
**S. Vahidinia**, J.N. Cuzzi, M. Hedman, B. Draine, R.N. Clark, T. Roush,  
G. Filacchione, P.D. Nicholson, R.H. Brown, B.J. Buratti, C. Sotin
- 11:40-12:00 *Is the F ring a Dusty Plasma?*  
**F. Crary**
- 12:00-13:40 **Lunch**

## Friday Afternoon, July 29

---

- 13:40-14:00 *Origin of Saturn's Rings via Tidal Stripping from a Lost Titan-Sized Satellite*  
**R.M. Canup**
- 14:00-14:20 *Satellite Formation in the Aftermath of the Formation of Saturn's Rings*  
**S. Charnoz**, V. Lainey, A. Crida
- 14:20-14:40 *The Origin of Saturn's Rings*  
I. Mosqueira, **P.R. Estrada**
- 14:40-15:00 *Viscous Spreading of Dense Planetary Rings*  
**J. Salmon**
- 15:00-15:20 **Break**
- 15:20-15:40 *The Rate of Impacts on Saturn's Rings*  
**L. Dones**, E.B. Bierhaus, Jr., J.L. Alvarellos, K.J. Zahnle
- 15:40-16:00 *Modeling the Long Term Evolution of the C ring Due to Ballistic Transport.*  
**P.R. Estrada**, R.H. Durisen
- 16:00-16:20 *The Ballistic Transport Instability Revisited*  
**H. Latter**
- 16:20-16:40 *Observations of Ejecta Clouds Produced by Impacts onto Saturn's Rings*  
**M.S. Tiscareno**, C.J. Mitchell, C.D. Murray, D. DiNino, J.A. Burns,  
M.M. Hedman, K. Beurle, M.W. Evans, C.C. Porco
- 16:40-17:00 *A Post-Equinox View of Saturn's Rings*  
**L.W. Esposito**
- 17:00-18:00 **Discussion**

## Wednesday Morning

---

### **Revisiting the Self-Gravity Wakes Granola Bar Model: More Data, More Parameters**

*Joshua E. Colwell, Richard G. Jerousek, James H. Cooney*

Colwell et al. (2006) presented a simple rectangular slab model of self-gravity wakes in Saturn's rings that matched variations in observed optical depth in UVIS stellar occultations due to varying viewing geometries with respect to canted opaque self-gravity wakes. Hedman et al. (2007) presented a similar model with wakes of elliptical (rather than rectangular) cross-section that provided a better fit to CIRS azimuthal scans the granola bar model of Colwell et al. (2006). Those early analyses were based on a relatively small number of occultations. With over 100 UVIS stellar occultations at a wide range of observing angles, we now revisit the granola bar model with an additional softening parameter at the edge of the wakes.

In addition to opaque wakes separated by translucent gaps with a finite non-zero optical depth, we now have a transition region between the gap optical depth and the wake optical depth (assumed to be infinite) represented by a truncated Gaussian profile in optical depth as a function of the cross-wake dimension. We applied this model to our observations with good signal. Then, based on the returned self-gravity wake parameters in the A and B rings, we use the same model to calculate predicted line-of-sight optical depths for all possible viewing geometries across the ring system. This look-up table of optical depth can be used in modeling of thermal emission and reflectance observations of the rings (Bradley et al. 2011, this workshop).

### **Self-Gravity Wakes and the Viscosity of Dense Planetary Rings**

*Glen R. Stewart*

Many features in Saturn's B ring, including large-scale radial structures, sharp gradients, and the strange behavior of its outer edge all suggest that dense rings exhibit strong deviations from what would be predicted for a simple viscous fluid. Local N-body simulations show that the effective viscosity in dense rings is dominated by gravitational interactions between elongated clumps of particles, the so-called self-gravity wakes. The radial separation between self-gravity wakes scales as the Toomre wavelength, which is linear in the surface density. However, N-body simulations show that as the surface density is increased, the self-gravity wakes become wider and the remaining clear space between them becomes narrower. A linear theory for the gravitational interaction between neighboring self-gravity wakes has been derived using the analogy of the two-stream instability in plasma physics. The theory predicts that the gravitational interactions are highly shear-dependent and become weaker when the separation between the adjacent wakes becomes too small. These results suggest that the effective viscosity is strongly shear-dependent and may have an unexpected dependence on surface density. A strongly shear-dependent viscosity implies that dense rings are a non-Newtonian viscous fluid that can exhibit the kind of shear-banding instabilities that are more commonly found in complex polymer fluids. The resonantly perturbed B ring edge is subject to a time variable shear rate and surface density, which is likely to lead to viscoelastic behavior. The theory can also be used to explain irregular structures in the F ring that may be caused by gravitational interactions between adjacent strands in the ring. High-resolution observations of the F ring may therefore provide a valuable test of the theory.

## Wednesday Morning

---

### **B ring gray ghosts in Cassini UVIS occultations**

*M. Sremčević, L.W. Esposito, J.E. Colwell, N. Albers*

In this paper we show results of a new analysis of the smallest scale ring structure in Cassini UVIS occultations. Comparing single occultation measurement of optical depth at time  $T_0$  with the next sample  $T_0 + dT$  (dozen meters in the ring plane) we build a map of transition probabilities of the ring structure. This allows us to view the ring structure as Markov system and examine (quasi) absorbing states.

The A ring occultations are easiest to interpret and are consistent with published models. The ring is composed of the two absorbing states corresponding to nearly opaque wake and transparent gap. Thus, the ring is constantly flipping between opaque and transparent state. The C ring shows only one absorbing state, consistent with the absence of self-gravity structure. Additionally we find a very small probability of the ring to be nearly transparent (so called “ghosts”). In other words, the ring is boringly homogeneous for most of the time, except for occasional narrow gaps.

The B ring results are the most puzzling. Following the published papers we were expecting qualitatively similar picture as in A ring: opaque self-gravity wakes and (nearly) transparent gaps. Which then implies two absorbing states. However, only a single absorbing state of very high optical depth ( $\tau > 4$ ) was found. In addition to this one absorbing state, the ring shows occasional brief transitions to states of relatively lower optical depth ( $\tau$  of 1 or 2, dubbed “gray ghosts”). However, the ring very quickly returns to the nominal absorbing state of very high optical depth. In other words, B ring is mostly in a high optical depth state and occasionally flips for a very short period of time to gray ghosts. The ephemeral gray ghosts are too infrequent to be playing the role of the expected transparent gaps, and are certainly not transparent. Up to now not a single published N-body simulation of the B ring matches our observations. However, we note a tendency that simulations with smaller surface density show fewer low optical depth regions, thus coming closer to the observed UVIS results.

### **Simulating the B ring**

*Mark Lewis*

One of the most significant open questions related to the rings of Saturn is their total mass, most of which is in the B ring. The lack of density waves in most of the B ring means that it is far harder to establish a surface density there than it is for the A ring. To further complicate matters, numerical simulations have shown that as more particles are added, gravity wakes tend to lead to clumping of particles in ways that doesn't agree with occultations which show that effectively no light gets through the densest parts of the B ring. To help understand what is going on, simulations of the B ring are performed which use surface densities of 600 g/cm<sup>2</sup> and higher with geometric optical depths that get into double digits to see what happens in those situations.

## Wednesday Morning

---

### **Noncircular features in Saturn's Rings: I. The Cassini Division**

*R. G. French, P. D. Nicholson, J. Colwell, E. A. Marouf, N. J. Rappaport, M. Hedman, K. Lonergan, C. McGhee-French, and T. Sepersky.*

Although Saturn's rings appear at first glance to be axisymmetric, more precise measurements reveal that many of the gap edges and narrow ringlets within the rings are in fact noncircular. We present preliminary results from a comprehensive study of noncircular features in the Cassini Division, based on occultation data from the Cassini mission. The simplest noncircular features can be modeled as inclined Keplerian ellipses, freely precessing under the influence of Saturn's oblate gravity field. These include the four dense ringlets that inhabit the Huygens, Herschel and Laplace gaps, three of which also have measurable inclinations with respect to the mean ring plane. In addition to simple eccentricities, we also find a surprisingly rich assortment of normal modes on the edges of both ringlets and gaps, some with as many as three or four normal modes coexisting at a single edge with comparable amplitudes. Our fits also reveal the pervasive effects of the strong Mimas 2:1 inner Lindblad resonance (ILR): nearly all of the sharp-edged features in the Cassini Division exhibit a small but detectable  $m = 2$  variation whose apoapse is locked to Mimas. The amplitudes of these distortions decrease with distance from the resonance, and nicely conform to a simple analytical model for isolated test particles perturbed by the resonance.

### **Noncircular Features in Saturn's Rings: II. The C Ring**

*P. D. Nicholson, R. G. French, M. M. Hedman, E. A. Marouf, J. E. Colwell, N. Rappaport, T. L. Sepersky and K. R. Lonergan*

Since the Voyager encounters in 1980/81, it has been known that many of the narrow ringlets within Saturn's rings are noncircular, a characteristic they share with the narrow uranian rings. We present preliminary results from a comprehensive study of noncircular features in the C Ring, based on Cassini occultation data.

In agreement with past studies, we find that the Colombo (or 'Titan') ringlet precesses at the same rate as Titan's mean motion, with an apoapse oriented to within 4 degrees of Titan's mean longitude. We thus confirm that this ringlet is locked in the Titan 1:0 inner Lindblad resonance. However, the new data show that both edges of this ringlet also exhibit free normal modes, with  $m = 0$  on the inner edge and  $m = 2, 3$  and 4 on the outer edge, with amplitudes ranging from 1.0 to 4.0 km. By contrast, the Maxwell ringlet freely-precesses at a rate which is consistent with that predicted from Saturn's zonal gravity harmonics. This ringlet exhibits an unusually large eccentricity gradient, comparable to that of the uranian epsilon ring. In this case, we see no evidence for additional normal modes on either edge. Neither the Maxwell nor Titan ringlet has a measurable inclination wrt the mean ring plane.

Our fits show that the Bond ringlet's outer edge is perturbed by the Prometheus 2:1 ILR, with an amplitude of 1.2 km and a pattern speed equal to the moon's mean motion. The ringlet's inner edge appears to be circular. The inner edge of the 20 km-wide Dawes gap coincides with the Mimas 3:1 ILR, and we indeed find evidence for a resonantly-forced  $m = 2$  perturbation with an amplitude of 5.2 km, matching the predicted pattern speed. But this is superimposed on a freely-precessing ellipse with an amplitude of 5.9 km.

## Wednesday Morning

---

### **Analysis of Saturn's Huygens Ringlet using Cassini ISS images**

*J.N. Spitale, C.C. Porco, J.M. Hahn*

We examine Saturn's Huygens ringlet using 5 years of Cassini ISS images. We find  $m = 2$  patterns on the inner and outer edges, moving at different speeds. The 1.6-km inner pattern moves at Mimas' speed and is presumably a response to the 2:1 Lindblad resonance. The speed of the 3.0-km outer pattern indicates that it is a free oscillation.

The relation between Keplerian modes of the inner and outer edges of the ringlet is complicated, with two distinct behaviors apparent: the earliest data set, taken in 2005, shows a steep eccentricity gradient, a mean width of  $\sim 50$  km, and an apsidal offset (outer minus inner) of  $\sim 45^\circ$ ; later data sets show a nearly flat eccentricity gradient, mean widths decreasing with time to  $\sim 20$  km, and near apsidal alignment.

Differential precession would produce a negative apsidal offset (at least initially), not the positive offset seen in the earliest observation. In order to reach the observed configuration, the ring would have to be either oscillating about an apse-aligned state with an amplitude of at least  $45^\circ$ , or the inner edge would need to have overtaken the outer edge shortly before the 2005 observations. In order for the inner apoapse to shear past the outer periapse, the ring elements would need to adjust to avoid streamline crossing. The large mean width and eccentricity gradient seen in the earliest data set may be consistent with such an adjustment. The decreasing width seen in the subsequent observations suggests an active confinement mechanism that has yet to be explained.

### **Global N-body Integrations of Planetary Rings**

*Joseph M. Hahn and Joseph N. Spitale*

A planetary ring that is disturbed by a satellite's resonant perturbation tends to respond in an organized way. When the resonance lies in the ring's interior, the ring responds via an  $m$ -armed spiral wave, while a ring whose edge is confined by the resonance exhibits an  $m$ -lobed scalloping along the ring-edge. The amplitude of these disturbances are sensitive to ring surface density and viscosity, so modeling these phenomena can provide estimates of the ring's physical properties. However a brute force attempt to simulate a ring's full azimuthal extent using a traditional N-body code is difficult due to the large number of particles needed to resolve the ring's behavior. Another impediment is the gravitational stirring that will occur among the simulated particles, which can wash out the ring's organized response. However it is possible to adapt an N-body integrator so that it can simulate a ring's collective response to resonant perturbations. The code developed here uses a few thousand massless particles to trace streamlines within the ring. Particles are close in a radial sense to all these streamlines, which allows streamlines to be treated as straight wires of constant linear density. In this approach, ring gravity is now a simple function of the particle's radial distance to all streamlines. And because particles are responding to smooth gravitating streamlines, rather than lumpy particles, this method eliminates the stirring that ordinarily occurs in brute force N-body calculations. Note also that ring surface density is now a simple function of streamline separations, so effects due to ring pressure and viscosity are easily accounted for as well. A poster will describe this N-body method in greater detail. Simulations of scalloped ring-edges, as well as narrow ringlets, are now executed in tens of minutes on a desktop PC, and results for the outer edge of Saturn's B ring and the nearby Huygens ringlet will be presented at conference time.

## Wednesday Morning

---

### **The Core of Ring F and New Corrugation Structure in Ring C**

*E. Marouf R. Franch, N. Rappaport, K. Wong, C. McGhee-French, A. Anabtawi*

Rich small-scale structure is revealed in Cassini radio occultation (RSS) profiles of Saturn's rings reconstructed to remove diffraction effects at radial resolution approaching few hundred meters. Two prominent examples are the  $\sim 1$  km wide core of Ring F and a recently uncovered quasi-periodic  $\sim 1.3$  km wavelength structure in inner Ring C. The tens of kilometers wide Ring F other Cassini instruments observe is undetectable by RSS, indicating lack of abundance of particle sizes exceeding few millimeters. When detectable, Ring F is almost always a single strand  $\sim 1$  km wide populated by centimeters and larger particles, hence likely the tracer of most mass (core). Surprisingly, this core is discontinuous, detectable in only 13 out of 44 Ring F crossings. Yet, dynamically it is well modeled by freely-precessing inclined Keplerian orbit (RMS residuals  $< \sim 7$  km). The Ring C structure, on the other hand, is quasi-periodic and extends hundreds of kilometers over 4 sub-regions of the innermost  $\sim 4000$  km. It modulates a tenuous background optical depth of  $\sim 0.05$  and has peak-to-peak fluctuations  $< \sim 0.01$ , making detection possible in only 3 recent RSS occultations conducted when the ring opening angle was  $< 5$  degrees. The structure is characterized by two interfering tones of spatial wavelength  $\sim 1.3$  and  $\sim 1.2$  km. The wavelength increases slowly with ring radius. The behavior appears consistent with presence of vertical corrugations 4-10 meters in height likely caused by a past ring tilting event and subsequent differential nodal regression of particle orbits. The corrugations model was proposed by Hedman et al. [Science 332, 2011] to explain intriguing 30-50 km wavelength structure observed in Cassini images (ISS) across Ring C. The RSS wavelength-radius behavior is in general agreement with the corrugation model prediction, however, important differences persist (ring mass effect?). The much shorter RSS corrugation wavelength compared with ISS implies a separate ring tilting event that is older by  $\sim 600$  years (late 1300's), and the two tones separation suggests two sub-events  $\sim 50$  years apart.

## Wednesday Afternoon

---

### **The Rings of Uranus: Shepherded, or Not?**

*Mark R. Showalter*

The rings of Uranus are widely suspected to be confined by the shepherding effects of small moons. Four resonances have been identified: Ring epsilon falls between Cordelia's 24:25 outer Lindblad resonance (OLR) and Ophelia's 14:13 inner Lindblad resonance (ILR). Cordelia's 23:22 ILR falls atop ring delta and its 6:5 ILR atop ring gamma. Other ring edges are unexplained. In addition, painstaking analysis of occultation data has revealed radial modes operating in two rings: a two-cycle oscillation ( $m=2$ ) in ring delta and a "breathing" mode ( $m=0$ ) in ring gamma. Finally, ring lambda comprises a co-rotating pattern of five uniformly-spaced arcs. These patterns remain unexplained.

If an optically thick ring varies in width due to a resonant or non-resonant mode, then its radially integrated reflectivity should show periodic variations travelling at the associated pattern speed. The expected resonant patterns in ring epsilon, with  $m=24$  and  $m=14$ , were first noted in Hubble images of the Uranian rings in 2006. In a quick re-analysis of six wide-angle Voyager images, these patterns are stunningly obvious, and the other known patterns are easily detected. This fine sensitivity raises the possibility that any additional patterns with  $m$ -values up to a few hundred should be detectable in each ring. The initial analysis already suggests the presence of a previously unidentified  $m=4$  pattern in ring gamma, which is superimposed upon the  $m=6$  pattern driven by Cordelia.

I will report on the results of a comprehensive analysis of the finest-resolution Voyager images. If shepherding plays a role in the other Uranian rings, then it should be possible to identify the associated resonant patterns even if the moons themselves are too tiny to have been revealed by Voyager's cameras.

### **The Activity of Spokes in Saturn's B Ring**

*Colin Mitchell, Carolyn Porco, Luke Dones, Joe Spitale*

We examine the spoke activity level in Saturn's B ring, defined as the area integrated optical depth of the spokes, for periodicities and correlations with magnetic longitude to determine any possible connections to Saturn's magnetosphere. We calculate the power spectrum of spoke activity in Cassini observations taken in the extended mission, and find a peak in the spectrum near 637 minutes, similar to Voyager measurements. We also calculate the spoke activity as a function of longitude in coordinate systems rotating with various constant periods near the SKR period and determine the degree of organization. From this we calculate a spoke activity-based coordinate system, locate the spoke active sector within it, and predict the location of the northern SKR active sector at the time of our observations near equinox.

Individual spoke activities observed to increase or decrease as a function of time, with few spokes maintaining a constant activity. Additionally, some spoke edges are observed to orbit at rates between Keplerian and corotation. We use the variation from Keplerian to calculate the charge to mass ratio necessary for a particle to orbit at that rate. Additionally, we measure the shear rates of the spoke edges.

## Wednesday Afternoon

---

### **The Structure of Saturn's E ring as seen by Cassini CDA**

*S. Kempf, R. Srama, G. Moragas-Klostermeyer, F. Postberg, J. Schmidt and F. Spahn*

The Cassini onboard dust detector measures the mass, speed, charge, and composition of individual ring particles. Thus, the size and speed distribution of the E ring particles can be derived from CDA measurements obtained during Cassini's ring traversals. Because there is an intimate connection between the ring particle dynamics and the distribution of the ring particle speeds, CDA provide precious information about the processes sculpting the ring. Here we present speed and size distributions measured inside and outside the orbit of the dominating ring particle source, the active ring moon Enceladus. We also present radial density profiles of the inner E ring obtained during equatorial ring traversals, which show a pronounced dependence of the ring structure on the hour angle.

### **The E Ring Re-imaged and Re-imagined**

*J.A. Burns, M.M. Hedman, D.P. Hamilton, M.R. Showalter*

Saturn's diffuse E ring consists of many micron-sized grains of water ice distributed between the orbits of Mimas and Titan. Various gravitational and non-gravitational forces perturb these particles' orbits, causing the ring's local particle density to vary noticeably with distance from the planet, height above the ring-plane, hour angle and time. Using remote-sensing data obtained by the Cassini spacecraft in 2005 and 2006, we investigate the E-ring's three-dimensional structure during a time when the Sun illuminated the rings from the south at a high elevation angle ( $> 15^\circ$ ). These observations show that the ring's vertical thickness grows with distance from Enceladus' orbit and its peak brightness density shifts from south to north of Saturn's equator plane with increasing distance from the planet. These data also reveal a localized depletion in particle density near Saturn's equatorial plane around Enceladus' semi-major axis. Finally, variations are detected in the radial brightness profile and the vertical thickness of the ring as a function of longitude relative to the Sun. Possible physical mechanisms and processes that may be responsible for some of these structures include solar radiation pressure and electromagnetic perturbations associated with Saturn's shadow.

### **Circumplanetary Dust in Multipolar Magnetic Fields**

*D. Jontof-Hutter and D.P. Hamilton*

Micrometeoroid impacts on small moons or ring particles produce debris of all sizes. Grains launched from parent bodies on initially circular orbits become electrically charged through interactions with plasma and sunlight. The motion of sub-micron dust grains is dominated by gravity and EM forces; collisions between dust grains are rare enough to be ignored. Depending on their launch distance and charge-to-mass ratio, some grains are unstable to radial perturbations (positively-charged grains only), while others are vertically unstable (positive and negative charges). These instabilities act on short timescales and can cause grains to collide with the planet or escape in less than one orbit. We have explored the boundaries between stable and unstable trajectories in detail for the idealized problem of a dipolar magnetic field centered and aligned with the rotation axis of the planet (Jontof-Hutter & Hamilton 2011).

Real planets, however, have more complex magnetic field configurations. Saturn's full magnetic field can be represented by a dipole offset northwards along the axis of rotation. This gives grains launched in the ring-plane an initial displacement from the magnetic equator. Jupiter's multi-polar field is dominated by a moderately tilted dipolar component. For both planets, the more complex magnetic fields increase the range of launch distances and grain sizes that are vertically unstable, but leave radial stability boundaries largely unaffected. On longer timescales, however, off-axis magnetic field components trigger destabilizing resonances with a grain's vertical or epicyclic motion, increasing radial excursions and allowing even negative grains to escape.

## Wednesday Afternoon

---

### **Evolution of Circumplanetary Dust Orbits at High Eccentricity due to Resonant Charge Variations**

*Les Schaffer*

We extend previous work on resonant charge variations (RCV) and their effect on orbital evolution of circumplanetary dust grains with an analytical and numerical study at large eccentricity  $e$ . Previous work has shown that in the limit of small  $e$  the dominant time variation in a grain's charge  $q(t)$  is at the grain's orbital period, and a resonant interchange of energy and momentum takes place via the Lorentz force between the rotating magnetic field and the charged grain. For large eccentricity the spectra of  $q(t)$  is more complex and the evolution rate is consequently altered. Variations in  $q$  are typically small enough that the grain charging equation can be linearized even for large  $e$ . The resulting evolution can then be computed by averaging RCV effects over one orbit. We map out  $\dot{a}$  and  $\dot{e}$  for a large range of  $a$  and  $e$  and typical plasma parameters. We display numerical simulations which qualitatively – and over a broad range in  $e$  quantitatively – confirm the analytical results. We next show that orbital evolution due to RCV is  $O(i^2)$ , and indicate how the theory can be extended to include finite  $i$ . We then numerically simulate passage through the  $l = 3$  inner Lorentz resonance (LR) at Jupiter to demonstrate that RCV can act in some cases so as to dampen the large induced  $e$  on resonance passage. This effect resolves an issue with earlier explanations of the Jovian ring halo structure near the resonance zone. Finally we discuss the sensitivity of RCV evolution rates to plasma charging models, and point out a weakness in the theory for grain charging currently in use. Nevertheless our analytical method is shown to be applicable to a range of plasma charging models.

### **Chaotic Dust Orbits at Uranus may Explain Hemispherical Color Asymmetries Common to its Regular Satellites**

*Daniel Tamayo, J.A. Burns, D.P. Hamilton, P.D. Nicholson*

When [1] noticed that Uranus' four largest moons had leading-trailing hemispherical color asymmetries, they conjectured that infalling dust from yet-to-be discovered, retrograde irregular satellites might be responsible. Eight such retrograde moons have since been found, and the recent detection of Phoebe's ring at Saturn [2] suggests that large dust rings generated by irregular satellites might be common around the giant planets. We therefore investigate whether infalling dust in the Uranian system might explain the color dichotomies among its regular satellites. In particular, we aim to understand why dust seems to have been distributed among them all rather than concentrated almost exclusively on the outermost moon, Oberon, as in the Saturnian case of Iapetus [3]. When studying the orbits of evolving dust grains, we find that Uranus' unique, extreme obliquity ( $98^\circ$ ) results in chaotic, large-amplitude variations in orbital eccentricity and inclination due to the wide misalignment between perturbations from the planet's oblateness and tidal perturbations from the Sun. These rapid orbital variations allow dust to access all the regular satellites simultaneously (rather than in sequence from outermost inward). This can explain the fact that all four moons exhibit leading-trailing hemispherical color asymmetries.

[1] Buratti, B.J., and Mosher, J.A. 1991, *Icarus*, 90, 1.

[2] Verbiscer et al. 2009, *Nature*, 461, 1098.

[3] Tamayo et al. 2011, *Icarus*, accepted for publication.

## Wednesday Afternoon

---

### **Plasma Variations in Saturn's Inner Magnetosphere from the Main Rings to Enceladus**

*M.K. Elrod, W. L. Tseng, R.E. Johnson*

With the discovery of an oxygen atmosphere over Saturn's main rings by the Cassini spacecraft observation (Tokar et al., 2005; Johnson et al. 2006), as well as a strong, but variable source from the plumes emanating from the southern polar region of the moon Enceladus (Porco et al., 2005; Smith et al., 2010) the physics of the inner magnetosphere from the main rings to inside the orbit of Enceladus has changed dramatically. This region contains  $O_2$  produced by the ring atmosphere and water group ions from the plumes. During the Saturn Orbit Insertion (SOI), July 1, 2004, Cassini detected a significant density of  $O_2^+$  ions over the main rings and between the F & G rings suggestive of an oxygen atmosphere produced from photochemistry of the ice particles in Saturn's ring system (Johnson et al., 2006, Tseng et al., 2009, Tseng & Ip 2010). We have produced a simple photochemistry model combining the water products from Enceladus and the seasonal effects on the ring atmosphere. The purpose of this study is to examine ion densities and composition from several periapses passes from 2004 to 2010 for the region in order to separate contributions from the seasonal effect on the ring atmosphere from any contribution from water products coming from Enceladus. Due to the high background of this region, the number of orbits used in this study with good pointing into the plasma is limited to 6 passes, SOI, 2005(Sept 5), 2007(June 11, June 27/28), and 2010 (Mar 3, June 19). Our analysis indicates a large variation in ion density and temperature between 2004 and 2010 and between the Voyager 2 data. Although the Enceladus plumes are variable, the very large variability in the ion density and the changing composition from 2004 to equinox appears to be more consistent with the seasonal variation estimated for the ring atmosphere.

## Thursday Morning

---

### **Scattering Properties of Saturn's Rings in the Far Ultraviolet from Cassini UVIS Spectra**

*E Todd Bradley, Joshua E Colwell, Larry W Esposito*

Physical properties of Saturn's rings such as the ring particle albedo, the mean path length a photon travels within a ring particle, and the ring particle phase function are poorly constrained in the FUV. Main ring spectra show an absorption feature due to water ice at 165 nm. We compared I/F values averaged above and below the absorption feature to the classical Chandrasekhar (1960) radiative transfer model for the C ring and the Cassini Division. For the A and B rings we replaced the scattering function from the Chandrasekhar equation with a self-gravity wake model for the A and B rings derived from stellar occultations (Colwell et al. 2006, 2007). The free parameters were the ring particle bond albedo ( $A_b$ ) and the ring particle asymmetry parameter ( $g$ ). We find  $A_b=0.06-0.09$  at 175-185 nm and  $A_b=0.02$  at 152-158 nm throughout the rings. Values of  $g$  range from -0.66 to -0.77 at 175-185 nm and from -0.68 to -0.81 at 152-158 nm showing that the ring particles are highly backscattering in the FUV. Small shifts in the wavelength of the absorption feature can be explained by differences in the photon mean path length,  $L$ . We scaled I/F from 152-185 nm to a spectral albedo model (Shkuratov et al 1999) to retrieve  $L$ . We found  $L$  is positively correlated with phase angle, which we attribute to multiple scattering within the particle on length scales smaller than  $L$ . We found values of  $L$  at zero phase angle from 2.0 to 2.5 microns which we interpret as twice the distance from the surface of a ring particle to the first scattering center.  $L$  is close to constant across the rings suggesting the outermost 1.25 microns of the ring particles have the same structural properties in all ring regions.

### **The Composition of Saturn's Rings from Cassini VIMS**

*Roger N. Clark, Jeff Cuzzi, Gianrico Filacchione, Dale P. Cruikshank, Philip D. Nicholson, Matthew M. Hedman, Robert H. Brown, Bonnie J. Buratti, Kevin H. Baines, and Robert M. Nelson*

Spectra of the rings of Saturn from Cassini VIMS, covering from 0.35 to 5.1 microns show unusual properties. Saturn shine contaminates many observations, except near the shadow of Saturn. Spectra uncontaminated by Saturn shine, selected as a function of phase angle from zero to 180 degrees, contain a wealth of information. At 180 degrees, no ice bands appear except for a feature in the F-ring near 3-microns where the index of refraction is unity. At phase angles near 180 degrees, weak ice absorptions appear and get larger with decreasing phase angle. The high phase observations contain no detectable particle to particle reflections. This indicates that the rings behave more like a fluid rather than separated moonlets. Spectra at low phase angles indicate a large range of ice grain sizes, from tens of microns to sub-micron. Sub-micron ice grains create unusual spectral properties, including decreased reflectance near 5-microns, decreased 3.1-micron Fresnel peak, decreased 2.6-micron reflectance, asymmetric long 2-micron absorption, reduced 1.5/2-micron ice band depth ratio, and enhanced reflectance at shorter wavelengths, all of which are seen in the VIMS spectra of the rings. In the blue/UV, spectra of the rings depart from that of ice by an as yet unidentified absorber. A number of materials have been proposed, including tholins and nano-hematite. Another possibility is nano-metallic iron as a Rayleigh absorber. Some spectra of Saturn's rings are very similar to spectra of some locations on Iapetus, where the evidence for mixtures of ice with nano-iron and nano-hematite are strong. If present, only a few tens of parts per million nano-iron is needed to explain the UV absorber in Saturn's rings.

## Thursday Morning

---

### **Saturn's Rings: What's the Red Stuff and How Much is There?**

*J.N. Cuzzi, S. Vahidinia*

Because Saturn's rings have almost certainly incurred intense structural evolution and redistribution on timescales short compared to any reasonable formation age, our best information about their origin is likely to come from their composition. That they are predominantly water ice is constrained primarily by a combination of decades-old microwave brightness temperature observations and radiative transfer models, although local mass densities are supportive. These Voyager-era studies all assumed classical many-particle-thick rings, in which the particles are well-separated and their scattering properties (reflectivity and emissivity) can be calculated with Mie theory and doubling codes. However, recent modeling (Vahidinia et al 2011) suggests that particle volume densities of 10% or more - such as almost certainly characterize at least the dense B and A rings - can have a strong effect on the reflectivity and emissivity of a particle layer, especially when many of the particles are wavelengths in size. Suggestions will be presented for future work. The distinctly reddish ring color has been ascribed to various organic materials, and more recently to nano-iron or nano-hematite, mixed with the dominant water ice. In addition, regionally varying amounts of a spectrally neutral absorber, carbon in particular, have been advocated to explain ring particle albedos quantitatively. We will discuss the properties of these classes of material with an eye to understanding how composition and/or grain size of pollutants might contribute to a reddish ring particle color, how the rings compare in this regard to other icy bodies, how the ring environment might be playing a role, how model assumptions come to bear, and how we might discriminate between the candidates.

Vahidinia, S., J. Cuzzi, B. Draine, and E. Marouf (2011); Radiative transfer in closely packed realistic regoliths; 2011 DPS meeting, Nantes.

### **Interactions of Saturn's Moons with its Ring System**

*Bonnie J. Buratti*

One of the main goals of the Cassini Mission is to understand the interactions between Saturn's system of rings and its moons. The saturnian system is unique in that there is substantial interaction between the rings and both small and the medium-sized satellites. At least three kinds of processes occur: feeding, accretion, and confinement of ring particles by the small inner satellites; deposition of E-ring particles - which themselves originate from Enceladus onto Mimas, Tethys, Dione, and Rhea; and the accretion of particles from the Phoebe ring from the leading side of Iapetus and perhaps Hyperion and even Titan. In addition, the main confinement mechanism of the rings and ringlets is resonances between the satellites.

The optical properties of the 'shepherd' satellites and the coorbitals are tied to the A-ring, while those of the Tethys Lagrangians are tied to the E-ring of Saturn. The color of the satellites becomes progressively bluer with distance from Saturn, presumably from the increased influence of the E-ring; Telesto is as blue as Enceladus (Buratti et al., Icarus 2010).

The giant Phoebe ring and its coating of the leading side of Iapetus may be a paradigm for other outer planet satellites. There is evidence that Oberon is being coated with an unseen ring of dust created by the outer irregular retrograde moons of Uranus, while Callisto may be the Iapetus of the Jovian system (Bell et al., 1985).

The study of the optical properties of the moons of Saturn offers clues to their interactions with the ring system, but the coating of satellites makes it difficult to understand geologic processes in terms of the optical properties of the surface.

Funded by NASA.

## Thursday Morning

---

### **Using Spectra to Probe the Densest Parts of Saturn's Rings**

*M.M. Hedman, P.D. Nicholson*

The Visual and Infrared Mapping Spectrometer (VIMS) onboard the Cassini Spacecraft has performed a number of moderately high-resolution (better than 200 km/pixel) spectral observations of Saturn's main rings. These data show that the rings' spectral properties vary on a broad range of spatial scales. Some of these variations reflect differences in the typical grain size in the ring particles' regolith, while others can be ascribed to different concentrations of impurities mixed with the ring-particles' water ice. VIMS has also observed many stellar occultations of the rings, which provide high-resolution profiles of the ring's opacity. Comparing these two data sets reveals a number of interesting correlations between the rings' spectral and structural properties on spatial scales between 100 and 1000 km. Such correlations provide new insights into how the surface properties of individual ring particles can be influenced by (and thus probe) the local dynamical environment.

In the A ring, we observe features in the spectral profiles at the locations of strong density waves. These features appear both in the ice-band depths and in the blue slopes, and thus likely reflect changes in the ring-particles' regolith properties. At the core of these features, which correspond to the locations of the waves themselves, the ice bands are enhanced, indicating larger typical grain sizes. Outside of this core, a more diffuse "halo" of reduced band depths can be observed, indicating smaller typical regolith grain sizes. These spectral signatures probably result from the enhanced collision frequencies within the density waves themselves. A similar form of dynamical heating may also be responsible for the few features in the B ring's spectral profile that do not appear to be correlated with optical-depth variations, which are also found in association with strong satellite resonances. These features may provide a new probe of the densest part of Saturn's rings

### **Mapping Ring Shadow Cooling and Thermal Inertia with Cassini CIRS**

*S. M. Brooks, L. J. Spilker and R. Morishima*

We use data from Cassini's Composite Infrared Spectrometer to characterize ring shadow cooling and to document radial variations in ring thermal inertia. CIRS records infrared radiation between 7 and 1000 microns. Far infrared radiation (16.7-1000 microns) is recorded at focal plane 1 (FP1). Thermal emission from Saturn's rings peaks at FP1 wavelengths. As shown in Spilker et al. (2005, 2006), ring thermal emission is well characterized as blackbody emission multiplied by a scalar factor related to the emissivity of the rings. Ring temperatures are generally warmer and the rings show significantly more thermal contrast at larger solar elevations.

The thermal budget of the rings is dominated by incident solar radiation. When ring particles enter Saturn's shadow this source of energy is abruptly cut off with a consequential decrease in ring temperature. To characterize this cooling, FP1 scanned the main rings repeatedly with a constant offset from the ingress shadow boundary in order to characterize this cooling. We show that shadow cooling is most significant in the C ring and Cassini Division. More modest cooling occurs in the B and A rings. From such shadow observations we create cooling curves at specific locations. By resampling the FP1 scans onto a common radial grid, we can document the cooling of the ensemble of ring particles as they enter Saturn's shadow. We will use a thermophysical model of the rings, such as that of Morishima et al. (2011), to derive particle thermal inertias from these cooling curves. Radial variations in thermal inertia can then be compared to other known variations in key ring parameters.

This research was carried out at the Jet Propulsion Laboratory, California Institute of Technology, under contract with NASA. Copyright 2011 California Institute of Technology. Government sponsorship acknowledged.

## Thursday Morning

---

### **On the Nature of the Scattering in Thermal Data of the Saturn's Rings**

*E. A. Deau, L. J. Spilker, R. Morishima and the Cassini CIRS Ring Team*

With the Prime, Equinox and Solstice missions, the Cassini Composite Infrared Spectrometer (CIRS) has acquired an extensive set of thermal measurements of Saturn's main rings (A, B, C and Cassini Division) in the thermal infrared. Temperatures were retrieved for the lit and unlit rings over a variety of ring geometries that include solar phase angle, spacecraft elevation and local hour angle. Temperatures were also retrieved at solar elevations ranging from 24 degrees to zero degrees at equinox.

To first order, the largest temperature changes on the lit face of the rings are driven by variations in phase angle while differences in temperature with changing spacecraft elevation and local time are a secondary effect. In the C ring, the thermal phase curves for a 1 degree-range of solar elevation typically show about a 5K scatter. By contrast, a similar scattering is noticed in the B ring, but is more reduced (less than 2K). The scattering is also observed in time curves (Temperature vs local time) and tilt curves (Temperature Vs spacecraft elevation), still for a 1 degree-range of solar elevation.

We propose a better understanding of the thermal scattering by simulating it with a thermal model as a function of the viewing geometry parameters and/or ring properties. We also investigate the nature of the thermal scattering as a noise resulting from the blackbody fit to the infrared spectra.

### **Modeling Thermal Transport and Emission of Particle Ensembles**

*Stuart Piorz*

Since 2004, Cassini's Composite Infra-Red Spectrometer (CIRS) has taken over a million spectra of Saturn's main rings. Almost all spectra are well fit with a Planck function and scalar multiplier, producing a database of effective temperature and emissivity that vary with location, illumination and viewing geometry.

Even a forward modeling of the emission is rendered difficult by computational hurdles and a multiplicity of parameters; although models are being brought into agreement with data, they suffer significant shortcomings. Ray tracing is too slow for proper sensitivity analyses, but classical radiative transfer provides questionable approximations; 3-d conductive heat flow is reduced to 1-d computations and/or reasoned approximations applicable to isolated moonlets. Extant models start with assumed ring structure and hone parameter values to consistency, but the models are not unique, and there is a phenomenological gap in extending from observed ring properties to particle properties. One example is the relation between the thermal inertia of a ring versus its constituent particles.

If thermal modeling of Saturn's rings is to be more than a consistency check, e.g., to constrain A-Ring wake parameters or draw tenable conclusions about heat transport through the B-Ring, then basic computational difficulties must be addressed. I present a model for the thermal transport and emission of an ensemble of particles that borrows from work in computer graphics and chip design to address computation of the radiation field. A ring section is modeled as layers of "checkerboards," with flat particles filling random locations. Thermal coupling and the multiple scattered light field are effected via a radiosity computation, where the number of neighbors exactly calculated relates to the density of a near-diagonal sparse coupling matrix. Merely using slab-like conduction can duplicate some features of observed ring emission, while the model allows a way to address and evaluate geometric and spin effects.

This work was performed at the SETI Institute under support from the NASA OPR Program.

## Thursday Morning

---

### **Modeling Saturn Ring Temperature Changes at Equinox**

*L. Spilker, C. Ferrari, R. Morishima*

The Cassini Composite infrared spectrometer (CIRS) retrieved the equinox temperatures of both sides of Saturn's main rings as the sun traversed from the south to north side of the rings. At equinox the rings are edge-on as seen from the sun and essentially edge-on (maximum ring opening of only about 2.5 degrees) as seen from Earth, so it is not possible to measure the main ring temperatures from Earth. At equinox the ring temperatures as a function of ring radius are almost identical on the north and south sides of the rings. The main rings cooled to their lowest temperatures measured to date.

Earlier in the mission, when the sun was the dominant heat source, the temperature of the lit rings decreased with increasing phase angle and the ring temperature in the shadow was less than the ring temperature at noon. At equinox the temperature does not decrease with increasing phase angle and the temperature at noon is no longer greater than the temperature in the shadow. To first order the temperatures are independent of phase angle demonstrating that the primary heat source is Saturn thermal and visible radiation. Current models are able to reproduce ring temperatures under Saturn heating only. More work is needed to understand their longitudinal variations.

## Thursday Afternoon

---

### **Particle Size Variations in Saturn's Rings from Occultation Statistics**

*Joshua E Colwell, James C Cooney, Larry W Esposito*

Showalter and Nicholson (1990) recognized that the sizes of particles in Saturn's rings affect the variance of the photon count rate in stellar occultations by the rings. Cassini UVIS stellar occultation data follow Poisson counting statistics in the absence of intervening ring material, or when the ring material can be approximated by a continuous medium with some finite optical depth. When particles or clumps of particles approach the scale of the spot of a singleintegration period, the variance increases. We present an analysis of Cassini UVIS occultation data statistics that shows significant differences in the excess variance between different ring regions and also between different occultation geometries with respect to the ring plane.

Among our findings are that the C ring plateaus have a qualitatively different behavior than the rest of the C ring, and that there is a region at the inner edge of the B ring that is distinguishable from the rest of the B1 region.

We developed a simple Monte Carlo model to generate synthetic occultation data for arbitrary ring particle size distributions. For a given size distribution we generate synthetic data over a range of optical depths,  $\tau$ , and compute the excess variance,  $\Delta\sigma^2$ , for each synthetic dataset. The resulting curves of  $\Delta\sigma^2$  as a function of  $\tau$  can then be compared to the data to provide some insight into the particle size distribution. However, the curves are not unique because a variety of particle size distributions can produce the same statistical properties in the data. Nevertheless, significant differences are seen between regions that point to underlying differences in the particle or clump size distribution. We will present the latest results of our analysis and modeling.

### **Measuring Centimeter-Sized Particles in the Saturnian Rings by Diffraction of Starlight**

*R. A. Harbison and P. D. Nicholson*

Occultations of Saturn's rings have proven to be a useful way to particle-size distribution of ring particles observed when in wavelength regimes where particles of different sized behave differently. French and Nicholson (2000) noticed in their stellar occultation work the presence of overshoots, places near a sharp edge of the rings, such as the Colombo, Maxwell, Huygens and Encke Gaps, where transmission of starlight appears to exceed unity. They attribute this to starlight scattered from the nearby ring into their detector.

The Cassini spacecraft, in orbit about Saturn, has also been measuring stellar occultations with the Visible-Infrared Mapping Spectrometer (VIMS), with over 70 occultations observed. Similar overshoots are seen in these data around gap edges in the A ring, C ring, and Cassini Division. They can be fit well by a simple diffraction model using centimeter-sized particles. We will present preliminary results on the particle-size distribution in the centimeter regime.

## Thursday Afternoon

---

### **Kinetics of Aggregation and Fragmentation - Size Distribution of Rings**

*F. Spahn, E. V. Neto, A.H. Guimaraes, N.V. Brilliantov, and A.N. Gorban*

A kinetic concept is presented covering coagulation and fragmentation of an aggregate ensemble including the combined dynamics of the mass spectrum as well as the velocity distribution of the aggregates. As a first step, based on the visco-adhesive collisional dynamics of two colliding particles, the aggregation- and fragmentation processes are described separately to allow estimation of the size spectrum. To this end we have assumed a Maxwellian for the velocity dispersion and use energy equipartition for simplicity. We obtain a generalized Smoluchovski-equation to quantify aggregation, which is limited to low impact-speeds.

This growth is counterbalanced by the fragmentation of colliding aggregates which occurs at higher collision speeds. A critical fragmentation speed is estimated by applying the dissipative collision dynamics and using energetic arguments; the gravitative - and adhesive binding energy.

A difficulty comprises of the size- and speed distribution left from a destructive collision. For the latter we again assumed a Maxwellian for simplicity. The mass spectrum was then estimated by simulating the fragmentation of two-dimensional agglomerates, held together by adhesive bonds, and then hit by an impacting projectile of given mass and impact energy. Both aggregates constitute of identical adhering spheres (constituents) forming a cubic lattice. A rather simple "random walk model" of crack-tip propagation has been studied numerically and analytically, where the breakage of adhesive bonds continues until the kinetic impact energy of the projectile is exhausted. A large number of repeated numerical breakage experiments have yielded a power law fragment distribution  $p(s) \sim s^a$  with  $a = -3/2$  ( $s$  - mean diameter of the aggregates). The distribution can be theoretically described by a one-dimensional random walk model to mimic the propagation of cracks. This 2D "toy-model" has to be extended to the three dimensions, e.g. applying a two-dimensional random walk of a crack tip vector in a 3D cubic constituent matrix.

The next step is to combine (numerically or analytically) the aggregation and fragmentation kinetics - a further generalized Smoluchovski-equation in order to obtain a steady state mass spectrum of the aggregate ensemble which will then be compared with data of Cassini experiments of Saturn's rings.

## Thursday Afternoon

---

### **A Kinetic Fragmentation and Coagulation Model for the Distribution of Particle Sizes in Saturn's Rings**

*N. V. Brilliantov, P. Krapivsky, H. Hayakawa, A. Bodrova, F. Spahn, and J. Schmidt*

We propose a new kinetic model for the evolution of the size distribution in a planetary ring, including coagulation and fragmentation of ring particles. Asymptotically the size-distribution approaches a power law with an exponential cut-off above a certain particle size, similar to the observed size distribution of Saturn's main rings.

Analysis of the light scattering properties of Saturn's rings suggests that the ring particles follow a steep size distribution  $p(r) \sim r^q$  that can be approximated by a power law with an exponent near  $q = -3$  (Zebker et al., 1985; French and Nicholson, 2000). The sizes are limited roughly to the range  $1 \text{ cm} < r < 10 \text{ m}$ , where the precise limits depend on the radial distance from Saturn.

Also a population of larger particles from  $r > 10 \text{ m}$  to a few hundreds of meters was inferred from the observation (Tiscareno et al., 2006, 2008; Sremcevic et al., 2008) of density signatures they induce in the ring (Spahn & Sremcevic 2000, Sremcevic et al., 2003). These larger particles probably exist only at certain distances from the planet and they obey a much steeper distribution with  $-6 > q > -9$ . Such an overall distribution of ring particles in form of a broken power law was proposed by Cuzzi et al., 1984.

It was suggested that the distribution of the smaller population may follow from a balance of coagulation and fragmentation, ring particles eventually forming fluffy aggregates called Dynamic Ephemeral Bodies (DEBs) (Davis et al., 1984).

The existence of the upper cut off in the distribution of the smaller (main) population of ring particles is still poorly understood. It was argued that the upper size cut off may result from tidal disruption, preventing further growth of aggregates larger than a certain size limit (Davis et al., 1984). However, even a minute tensile stress provided by adhesional sticking should allow for aggregate sizes well above 10 meters. On the other hand, Longaretti (1989) proposed an analytical model for the size distribution and argued that aggregates of size  $D$  would typically collide with each other at relative speeds ( $\Omega D$ ), so that a certain critical speed leading to disruption would correspond to a maximal size  $D$  of particles found in the ring. However, the aggregation kinetics, including the disruption and re-accumulation of the largest aggregates, was not modelled self-consistently in Longaretti's (1989) approach. The time-scale for their re-formation could easily be faster than the frequency of their mutual disruptive collisions, so that the argument does actually not hold.

Here, we propose a new model for the aggregation kinetics of Saturn's ring particles. We assume that ring particles consist of smaller building blocks, which tend to coagulate in low velocity collisions, forming gradually larger particles. At a certain small rate, however, collisions are assumed to be disruptive, releasing all building blocks from colliding aggregates. These disruptive collisions would correspond to the upper part of ring particles' speed distribution, with collisional kinetic energies sufficiently large to overcome an aggregate's binding energy. Alternatively, disruption may be provided by occasional destruction in meteoroid impacts on the rings.

We show that the system evolves to a power law size distribution with an exponential cut-off above a certain size, very similar to the observed one. The cut-off size depends in this case on the frequency of disruptive collisions relative to the frequency of coagulating collisions. The rate of restituting collisions (i.e. only energy loss, but no fragmentation and no sticking of particles) changes the timescale for the relaxation to the asymptotic size-distribution.

## Thursday Afternoon

---

### **OPUS: A Tool to Obtain Ring Data from the Planetary Data System**

*Mitchell K. Gordon, Lisa Ballard, Mark R. Showalter, Neil Heather*

We will demonstrate the use and capabilities of OPUS (Outer Planets Unified Search).

Identifying the specific data you need within the Planetary Data System has become more challenging with the huge increases in the amount of data held. The Planetary Rings Node holdings are approaching 1 Terabyte of data. OPUS is a powerful, form based tool at the Rings Node which allows users to search our holdings using a wide range of relevant parameters. We will describe how to quickly find the specific data you need.

OPUS currently supports searches for data obtained by three Cassini instruments (CIRS, ISS, VIMS), Galileo SSI, New Horizons LORRI (Jupiter encounter), Voyager 1 and Voyager 2 ISS. Work is underway to expand the coverage to additional instruments including HST observations that include the outer planets.

OPUS search results include preview images or footprint diagrams, and tables of information about each observation. These can be used to browse the search results and can be downloaded along with the selected data products. Recently added features include the capability to search for Cassini ISS movie sequences and the option to receive calibrated versions of Cassini ISS images returned by OPUS.

<http://pds-rings.seti.org/search/>

## Thursday Poster

---

### **The B ring edge: Impressions from Voyager ISS and Cassini UVIS**

*N. Albers, M. Sremčević, and L.W. Esposito*

Among the most striking discoveries during the Cassini mission are the structure and variability of the B ring edge which is directly influenced by the nearby Mimas 2:1 ILR.

Cassini UVIS data show the presence of structure on sub-km-scales in the region 50 - 150km radially inward of the edge. This structure correlates with the location of Mimas, and we find it to be the most abundant at +/-90 degrees from Mimas. Similarly, we find the optical depth to be consistent with the compression and decompression phase of the edge. Power or sub-km structure and maximum optical depth have been increasing as the effective edge pattern evolved into a more pronounced m=2 pattern thereby amplifying its radial excursion to more than 100km outward from resonance location. Most but not all of the variability in location can be described using the multi-mode model by Spitale and Porco (2010, SP2010 hereafter). Post-fit RMS residuals are 9.6km with a  $\chi^2/DOF$  of  $\sim 100$ .

Additionally, Voyager 1 and 2 ISS images provide a nearly complete azimuthal coverage of the edge and significantly expand its temporal coverage. The edge at Voyager epoch shows a clear two-lobed pattern with local disturbances similar to those reported from Cassini imaging, and best visible in Voyager 2 high-resolution images. Although the shape of the edge at this epoch is well-matched by the SP2010 model, the pattern is offset by  $\sim 80^\circ$  in corotating longitude. This shift is consistent with Mimas' offset in mean longitude due to its libration caused by the near-resonance with the moon Tethys. It seems that Mimas is dragging along the complete edge, including the "free modes" of SP2010, forcing the edge to follow Mimas' orbital changes.

## Thursday Poster

---

### **A Catalog of Features in Saturn's Rings from Cassini Occultation Observations**

*K. R. Lonergan, T. L. Sepersky, R. G. French, P. D. Nicholson, M. Hedman, J. Colwell, E. A. Marouf, N. J. Rappaport*

Saturn's ring system is replete with a host of ringlets, gaps, and other fine-scale structure, revealed at km-scale resolution in over 130 Cassini occultation observations. Using precise measurements of these features, we are able to determine the orbital properties of the rings to sub-km accuracy, determine the direction and precession rate of Saturn's pole, establish an accurate radius scale for the rings, and solve for the zonal harmonics of Saturn's gravity field. Here, we present a catalog of over 100 identifiable ring features. We illustrate our technique for accurately measuring their locations, and show representative radial optical depth profiles from Cassini RSS, VIMS, and UVIS occultations. The effective radial resolution of these data ranges from less than 100 m to 400 m, depending on sampling rate, SNR, and occultation geometry. Using a widget-based graphical user interface written in IDL, we can easily compare occultation profiles from the full set of Cassini occultation data, as well as historical Voyager 1 and 2 stellar and radio occultations, the widely-observed stellar occultation of 28 Sgr in 1989, and two HST stellar occultations in 1991 and 1995. Using these tools, over 20 undergraduate non-science majors (Team Cassini) at Wellesley College have contributed to the measurement of over 8000 individual ring occultation events, the raw material used for determining the geometry of Saturn's rings and determining the orbits of noncircular features in the rings.

### **The Geometry of Saturn's Rings from Cassini Occultation Observations**

*T. L. Sepersky, K. R. Lonergan, and R. G. French, P. D. Nicholson, M. Hedman, J. Colwell, E. A. Marouf, N. J. Rappaport and R. Jacobson*

Saturn's ring system is a complex dynamical laboratory, populated by a vast array of non-circular gap edges, narrow ringlets, and density waves revealed at km-scale resolution in over 130 Cassini occultation observations using the RSS, VIMS, and UVIS instruments. In order to take full advantage of the intrinsic resolution of the data, we must establish a highly accurate radial scale for each occultation. We begin with precise measurements of the observed times of sharp ringlet and gap edges in the occultation profiles, converted to radius in the ring plane using the reconstructed Cassini trajectory, and either star positions, corrected for proper motion and parallax at Saturn (for stellar occultations), or the planetary ephemeris, for RSS occultations. We then correct the radial scale of each occultation for small errors in the spacecraft trajectory, typically  $\sim 1$  km. This is done in an iterative fashion by identifying what appear to be "circular" features and using them to adjust the radius scale. We identify 26 such features in the Cassini Division, B and C rings; none are found in the A ring. Postfit rms residuals for these features are  $\sim 250$  m. This catalog of circular features is also used to determine the direction and precession rate of Saturn's pole, and corrections to the catalog star positions for earthbased stellar occultations. Using our final geometric solution, we are able to measure ring eccentricities ( $ae$ ) and inclinations ( $a \sin i$ ) as small as  $\sim 200$  m, and to detect normal modes in a host of ring features with comparable amplitudes. For some ring features, the rms residuals are as small as  $\sim 150$  m, a testament to the accuracy of the edge measurements and the overall accuracy of the trajectory corrections and the adopted ring orbit geometry. Ultimately, we anticipate that the absolute radius scale of the rings will be determined with an accuracy of better than 200 meters. This will provide an absolute reference system for detailed studies of density waves and other resonant phenomena, as well as for improvement in the measurement of Saturn's low-order gravitational harmonics.

## Thursday Poster

---

### **Effects of Inclination and Longitude of the Ascending Node of Gap Moons on Structure of Moon Wakes**

*Allyson Ducey and Mark Lewis*

We have seen that gap moons within Saturn's rings perturb the ring material on either side and create wakes on the edges of the rings. A parameter that has not yet been heavily investigated is the inclination of the gap moon; our research explores whether this orbital element contributes significantly to the wake structure. This is accomplished with the use of N-body spherical particle simulations with collisions and self-gravity that model the Keeler gap region of Saturn's rings. The simulations are input into a visualization program called SwiftVis, from which we can easily analyze different aspects of the resulting wake structure. In the simulations, the known characteristics of the Keeler gap and its moon Daphnis, such as eccentricity, mass, and width of the gap, remain at the observed values of  $e = 3.3 * 10^{-5}$ ,  $m = 8.4 * 10^{13}$  kg, and  $d = 42$  km, respectively. Characteristics which greatly affect the efficiency of the simulations, such as particle size, density, and optical depth of the ring material, are kept as accurate as the available computing power allows. Our simulations use  $r = 7.56$  m,  $\rho = 0.5$  g/cm<sup>3</sup>, and  $\tau = 0.2$ ; these values lead to particle simulations with  $N = 30$  million. Additionally, the simulations show whether the location of the longitude of the ascending node has any affect on the wake structure. In the future it may be possible to ascertain the location of the ascending node and compare its precession rate to expected values.

### **N-Body Simulations of Silicate Hiding In Saturn's Dense Rings**

*Gareth Jones and Mark Lewis*

Observations of the rings of Saturn show a mixed composition of mainly water ice and some contaminants. This concentration of water ice is interesting because the makeup of the rings reveals how they were formed. If they formed from an early moon that was ripped apart, the resulting rings would be different than if they formed from an icy centaur or formed at the same time as Saturn. The fact that the dense rings are characterized by gravity wakes, where particles clump together, allows for the possibility that they could hide higher density material. In order to determine how much contaminant material could be hidden in the dense rings, we ran N-body simulations for patches of ring particles varying the surface density and fraction of higher density particles. The output of these simulations was run through a ray-tracing photometry code to show how much of the contaminants would be visible. We show how this varies with lighting and viewing geometry.

## Thursday Poster

---

### **Fine-Scale Self-Gravity Density Wave Structure of Saturn's Main Rings**

*Evgeny Griv and Michael Gedalin*

We examine the linear stability of the Saturnian ring disk of mutually gravitating and colliding particles with special emphasis on its fine-scale of the order of 100 m density wave structure, that is, almost regularly spaced, aligned cylindric density enhancements and optically-thin zones with the width and the spacing between them of roughly several tens particle diameters. We analyze the Jeans' instabilities of gravity perturbations (e.g., those produced by a spontaneous disturbance) analytically by using the Navier-Stokes dynamical equations of a compressible fluid. A simple model of the system is considered consisting of a three-dimensional ring disk that is weakly inhomogeneous and whose structure is analyzed by making a horizontally local short-wave approximation. We demonstrate that the disk is probably unstable and that gravity perturbations grow effectively within a few orbital periods. We find that self-gravitation plays a key role in the formation of the fine structure, while interparticle collisions play a modest role. The predictions of the theory are compared with observations of Saturn's rings by the Cassini spacecraft and are found to be in good agreement. In particular, it appears very likely that some of the quasi-periodic microstructures observed in Saturn's A and B rings - both axisymmetric and nonaxisymmetric ones - are manifestations of these effects. We argue that the quasi-periodic density enhancements revealed in Cassini data are flattened structures, with a height to width ratio of about 0.3. One should analyze high-resolution of the order of 10 m data acquired for the A and B rings (and probably C ring as well) to confirm this prediction. We also show that the gravitational instability is a potential cluster-forming mechanism leading to the formation of porous 100-m-diameter moonlets embedded in the outer A ring, although this has yet to be directly measured.

### **Velocity Anisotropy-Driven Bending Instability in the Main Jovian Ring and Saturn's Faint D and C Rings**

*Evgeny Griv*

Galileo spacecraft images from 1996 and recent Cassini spacecraft images from 2007 to 2010 have revealed patterns of vertical corrugations in the main Jovian ring and Saturn's faint D and C rings. Different scenarios for tilting the rings have been explored by Burns, Hedman, Showalter, and others (e.g. impacts of external material, direct hits of large ring particles, atmospheric break-up and changes in Saturn's mass distribution that shift the planet's inertia tensor). Even though at the moment there are not enough data that would allow us to establish how common this feature in planetary rings, I tentatively relate these sinusoidal corrugations in the main Jovian ring and Saturn's D and C rings to the free bending transverse-type instability of gravity perturbations discussed in the present talk. The bending perturbations do not cause density enhancements. This type of the vertical, normal to the symmetry plane collective motions makes the ring disk bend in the same way as the plane of an oscillating membrane does. It is found that a vertical-to-plane anisotropy of random velocities of particles (or "pressure anisotropy") drives the instability: the disk would be unstable to the bending mode when the ratio of plane to vertical velocity dispersions exceeds about 2. The extent to which our results on the disk's stability can have a bearing on observable planetary rings is discussed as well.

## Thursday Poster

---

### **Cassini UVIS Observations of Saturn's Faint, Narrow Ringlets**

*Bryce Bolin, Josh Colwell*

The Cassini orbiter's Ultraviolet Imaging Spectrograph (UVIS) has observed a number of stars over 100 stellar occultations as they were occulted by various sections of the Saturn ring system. These stellar occultations are at a radial resolution of less than 20 m. Faint and narrow ringlets in the Colombo, Encke, G1, Huygens, Jeffreys, Laplace, and Maxwell gaps have been detected in ISS images and are seen in UVIS stellar occultation data. We have carried out a systematic search of UVIS occultation data for ringlets in these gaps. The following ringlets have been observed: R1 in the G1 gap, R2 in the Colombo gap, R6 in the Huygens gap, R8 in the Jeffreys gap, R9 in the Laplace gap and four faint ringlets found in the Encke gap. This analysis characterizes these ringlets in UVIS occultation data. A variety of azimuthal variations have been found in these ringlets in UVIS data including ringlet width, optical depth, radial profile and distance from Saturn. The Encke gap ringlets are only seen in some occultations indicating they are azimuthally discontinuous as also seen in Cassini images. In addition to measuring the equivalent widths and positions of the more prominent ringlets, a rigorous statistical test is applied to measurements of the faint R5 and R3 ringlets in the Huygens and Maxwell Gaps respectively. We were unable to detect these faint, dusty ringlets with confidence.

### **Dust-Plasma Interaction in the Rings of Saturn**

*Madeleine Holmberg, Jan-Erik Wahlund, Michiko Morooka, Shotaro Sakai*

The Cassini satellite has been orbiting Saturn since 2004 and are scheduled to do so until 2017. Measurements taken by the Cassini Radio and Plasma Wave Science (RPWS) instrument in the inner magnetosphere of Saturn have shown that dust-plasma interaction takes place between the E-ring particles and the surrounding plasma disk. We use Langmuir probe (LP) measurements from 130 orbits to map the structure and dynamics of the inner plasma disk of Saturn, the LP measurements are used to derive ion density and velocity. The mapping is done in order to reveal the degree and character of dust-plasma interaction in the region from 2.5 to 10  $R_S$ . The investigation shows that the plasma slows down due to the dust interaction within 6  $R_S$  near the equatorial plane where the spacecraft (dust) potential is negative.

## Thursday Poster

---

### **Thermal Inertia of Icy Particles of Saturn's Rings Inferred from Cassini CIRS**

*R. Morishima, L. Spilker, K. Ohtsuki*

The thermal inertia values of Saturn's main rings are derived by applying our thermal model to azimuthally scanned spectra taken by the Cassini Composite Infrared Spectrometer (CIRS). Model fits show the thermal inertia of ring particles to be 16, 13, 20, and 11 in MKS units for the A, B, and C rings, and the Cassini division, respectively. However, there are systematic deviations between modeled and observed temperatures in Saturn's shadow depending on solar phase angle, and these deviations indicate that the apparent thermal inertia increases with solar phase angle. This dependence is likely to be explained if large slowly spinning particles have lower thermal inertia values than those for small fast spinning particles because the thermal emission of slow rotators is relatively stronger than that of fast rotators at low phase and vice versa. Additional parameter fits, which assume that slow and fast rotators have different thermal inertia values, show the derived thermal inertia values of slow (fast) rotators to be 8 (77), 8 (27), 9 (34), 5 (55) in MKS units for the A, B, and C rings, and the Cassini division. The values for fast rotators are still much smaller than those for solid ice with no porosity. Thus, fast rotators are likely to have surface regolith layers, but these may not be as fluffy as those for slow rotators, probably because the capability of holding regolith particles is limited for fast rotators due to the strong centrifugal force on the surface.

### **Formation of a Propeller Structure by a Moonlet in a Dense Planetary Ring**

*S. Michikoshi*

The Cassini spacecraft discovered a propeller-shaped structure in Saturn's A ring. This propeller structure is thought to be formed by gravitational scattering of ring particles by an unseen embedded moonlet. Self-gravity wakes are prevalent in dense rings due to gravitational instability. Strong gravitational wakes affect the propeller structure. We derive the condition for formation of a propeller structure by a moonlet embedded in a dense ring with gravitational wakes. We find that a propeller structure is formed when the wavelength of the gravitational wakes is smaller than the Hill radius of the moonlet. We confirm this formation condition by performing numerical simulations. This condition is consistent with observations of propeller structures in Saturn's A ring.

### **Viscosity in Planetary Rings with Spinning Self-Gravitating Particles Obtained by N-body Simulation**

*Yuki Yasui, Keiji Ohtsuki, Hiroshi Daisaka*

We calculate ring viscosities using local N-body simulation, and examine effects of surface friction and the dependence of the viscosity on optical depth and distance from Saturn. First, we calculate viscosities in the case without surface friction. In the case of low optical depth, the viscosity was found to increase in proportion to the optical depth, and excellent agreement with the results based on three-body calculation was confirmed. However, in dense rings where gravitational wakes are formed, the results of N-body simulation deviate from the three-body results and the viscosity is significantly enhanced, in agreement with the previous results for rings with self-gravitating, smooth particles. Next, we examine the effect of surface friction and spins of particles. In the case of rings with low optical depth and weak self-gravity, both particle random velocities and viscosities are slightly lowered due to surface friction. On the other hand, in the case of optically thick rings in which wake structures are strongly formed, we found that the dependence of the viscosity on the tangential restitution coefficient is rather weak, indicating that the enhancement of the viscosity due to rings' self-gravity is much more significant than the effect of particles' surface friction. We will discuss a semi-analytic expression for ring viscosities based on our numerical results.

## Thursday Poster

---

### **Constraining Size Distribution in the F Ring**

*Tracy Becker, Joshua E. Colwell, Larry Esposito*

Data from the Cassini Mission to Saturn has supplied information about the planet's F ring with an unprecedented level of detail. This dynamically active ring is understood to be made up of fine particles as well as a narrow core of larger particles, clumps, and perhaps moonlets. Collisions between larger particles liberate smaller particles which provide most of the cross-section for remote-sensing observation of the rings. Here we describe a unique observation that provides insight into the smallest component of the F ring size distribution.

The solar occultation by the rings on Cassini rev 9 was observed by the Ultraviolet Imaging Spectrograph solar port at EUV wavelengths. In this particular occultation there was a misalignment of the Sun with the UVIS solar occultation field of view such that the direct solar signal was only 1% typical levels. Because of the misalignment, when the field of view was pointed at the F ring, the direct signal from the Sun was small, allowing us to measure an enhanced signal due to forward-scattering by the particles. There is a direct relationship between the amount of forward-scattered light and the size of the particles responsible for the scattering. We utilize this relationship in the model of the solar occultation that we are developing.

In our model we alter the sizes of the particles in the ring and measure the resulting amount of light scattered into the UVIS field of view. Using measured values for the optical depth in the region, we will be able to constrain the particle sizes in a portion of the F ring. The product of the model will provide a good constraint on the size distribution of this region of the F ring. Future solar occultations will be designed to replicate this geometry so that the measurement can be repeated.

### **Dynamical Stability of Saturn's F ring**

*A.D. Whizin, J.E. Colwell, J. N. Cuzzi*

Saturn's F ring has many dynamical features that vary on short timescales as observed in both Voyager and Cassini data because of perturbations by the F ring satellites Prometheus and Pandora (Murray, C. D., et al., 2008, *Nature*, 453, 7196, 739-744). The perturbations from these satellites place constraints on ring particles eccentricity growth and cause certain orbits in the F ring region to be chaotic (Winter, O. C., et al., 2007, *MNRAS*, 380, L54, and Winter, O.C., et al., 2010, *A&A*, 523, A67). Transient features in the ring (kinks, clumps, and other features (Esposito, L. W., et al., 2008, *Icarus*, 194, 278-289, and Charnoz, S., et al., 2005, *Science*, 310, 5752, 1300-1304)) suggest a population of unseen moonlets existing in the F ring. We present a new approach to study the dynamical stability of this moonlet belt. Specifically we examine the region of the F ring core to determine if it's in a location of long-term stability amongst the veritable sea of resonances with Prometheus and Pandora that exist there. We test our hypothesis that the F ring core has a dynamically stable, preferred location, between 140,150 km-140,250 km from Saturn. Using an N-body integrator and a simple perturbation model, we find a complex pattern of regions of relative stability between resonances with Pandora and Prometheus. We present results from two different numerical studies of the dynamical evolution of test particles within the F ring region. Perturbations of boulders and moonlets in the vicinity of the F ring region can cause them to collide with the F ring core providing a possible explanation for the ring's many complex transient features. Initial results show a correlation between the location of the core and regions of orbital stability.

## Thursday Poster

---

### **Capture of Irregular Satellites via Binary Planetesimal Exchange in Migrating Planetary Systems**

*Imran Hassan, Alex Moore, Alice Quillen*

By logging encounters between planetesimals and planets we compute the distribution of close approaches for planetesimals crossing planetary orbits in a two planet system that is migrating due to interactions with an exterior planetesimal belt. We find that close and slow encounters primarily occur with the outermost planet suggesting that outwards migrating outer planets could host captured irregular satellite populations. Taking care to consider where a planet orbit crossing binary planetesimal would first be disrupted we estimate the probability of both disruption and irregular satellite capture during disruption of a binary planetesimal. The probability is weakly dependent on outer planet mass and decreases with increasing outer planet mass. We estimate that the probability that the secondary of a binary planetesimal is captured and becomes an irregular satellite about a Neptune mass outer planet is about  $1/100 - 1/1000$  for binaries with masses and separations similar to those in the Kuiper belt. We discuss interpretation of emission associated with Fomalhaut b in terms of collisional evolution of a captured irregular satellite population.

### **Eclipses by Circumsecondary and Circumplanetary Disks and a Candidate Long and Deep Eclipse of a Pre-main Sequence Star in Sco-Cen**

*Eric Mamajek, Alice Quillen, Mark Pecaut, Fred Moolekamp, Erin Scott, Matt Kenworthy, Andrew Collier Cameron and Neil Parley*

The large relative sizes of circumstellar and circumplanetary disks imply that they might be seen in eclipse in stellar light curves. We estimate that a survey of  $\sim 10^4$  young ( $\sim 10$  million year old) post-T Tauri stars monitored for 10 years will display a couple of eclipses from circumplanetary disks and disks surrounding low mass companion stars. We present photometric data on a pre-main sequence K dwarf (1SWASP J140747.93-394542.6 = ASAS 140748-3945.7), a newly discovered  $\sim 0.9M_{sol}$  member of the  $\sim 16$  Myr-old Upper Centaurus-Lupus subgroup of Sco-Cen. This star exhibited a remarkably long, deep, and complex eclipse event centered on 29 April 2007 (as discovered in SuperWASP photometry, and with portions of the dimming confirmed by ASAS data). At least 5 multi-day dimming events of  $> 0.5$  mag are identified, with a  $> 3.3$  mag deep eclipse bracketed by two pairs of  $\sim 1$  mag eclipses symmetrically occurring  $\pm 12$  days and  $\pm 26$  days before and after. Hence, significant dimming of the star was taking place on and off over at least a  $\sim 54$  day period in 2007, and a strong  $> 1$  mag dimming event occurring over a  $\sim 12$  day span. We place a lower limit on the period of 850 days (i.e. the orbital radius of the eclipser must be  $> 1.7$  AU and orbital velocity must be  $< 22$  km/s). The shape of the light curve is similar to the lop-sided eclipses of the Be star EE Cep, and we suspect that this new star is being eclipsed by a low-mass object with an orbiting disk with significant substructure (thin dust debris belts or rings).

### **Stability of Multiple Planet or Satellite Systems**

*Alice Quillen*

We compute the strengths of zero-th order (in eccentricity) three-body resonances for a co-planar and low eccentricity multiple planet or satellite system. In a numerical integration we illustrate that slowly moving Laplace angles are matched by variations in semi-major axes among three bodies with the outer two bodies moving in the same direction and the inner one moving in the opposite direction, as would be expected from the two quantities that are conserved in the three-body resonance. A resonance overlap criterion is derived for the closely and uniformly spaced, equal mass system with three-body resonances overlapping when interplanetary separation is less than an order unity factor times the planet mass to the one quarter power. We find that three-body resonances are sufficiently dense to account for wander in semi-major axis seen in numerical integrations of closely spaced systems and they are likely the cause of instability of these systems. For interplanetary separations outside the overlap region, stability timescales significantly increase. Crudely estimated diffusion coefficients in eccentricity and semi-major axis depend on a high power of planet mass and interplanetary spacing. An exponential dependence previously fit to stability or crossing timescales is likely due to the limited range of parameters and times possible in integration and the strong power law dependence of the diffusion rates on these quantities.

## Friday Morning

---

### Small Propeller Signatures in the C Ring and Cassini Division

*K. Baillie, J.E. Colwell, L.W. Esposito*

We identified propeller-like signatures in Cassini UVIS stellar occultation data: we found evidence of the presence of holes in some regions of relatively high optical depth (typically ringlets or plateaus) in the Cassini Division and the C ring. These “ghosts” are characterized by an isolated peak in photon counts with a height equal to photon counts in places without ring material.

We suggest that our ghost observations are related to the presence of depletion zones that are opened on the outer trailing side and inner leading side of a small moonlet or boulder. These boulders are not massive enough to open full gaps, but could produce azimuthally limited holes in the rings like those seen in the UVIS occultation data and propeller features seen in the A ring by ISS and UVIS.

Even though these features are much smaller than the A ring propellers, we are able to measure the radial extent of the depletion zones. From previous models and numerical simulations of the interaction of a moonlet with ring particles, we are able to estimate a boulder size distribution that could be at the origin of our observations. Monte-Carlo algorithms allow us to remove the intrinsic bias of our data resolution, varying for each occultation based on navigation and geometry differences. We estimate that the ghosts we observe could be due to a boulder size distribution following a power-law with a cumulative index of -0.8 in the Cassini Division and -0.6 in the C ring, where Zebker et al. (1985, *Icarus* 64, 531-548) estimated power-law indices of -1.75 in the Cassini Division and -2.1 in the C ring, therefore suggesting the existence of populations of boulders in the C ring and the Cassini Division that are not part of the main population of ring particles.

### The Propeller and the Frog

*Margaret Pan*

“Propellers” in planetary rings are disturbances in ring material excited by moonlets that open only partial gaps. We describe a new type of co-orbital resonance that may explain the observed non-Keplerian motions of propellers. The resonance is between the moonlet underlying the propeller and co-orbiting ring particles downstream of the moonlet where the gap closes. The moonlet librates within the gap about an equilibrium point established by co-orbiting material and stabilized by the Coriolis force. In the limit of small libration amplitude, the libration period scales linearly with the gap azimuthal width and inversely as the square root of the co-orbital mass. The new resonance recalls but is distinct from conventional horseshoe and tadpole orbits; we call it the “frog” resonance, after the relevant term in equine hoof anatomy. For a ring surface density and gap geometry appropriate for the propeller Bleriot in Saturn’s A ring, our theory predicts a libration period of  $\sim 4$  years, similar to the  $\sim 3.7$  year period over which Bleriot’s orbital longitude is observed to vary.

## Friday Morning

---

### **Strands and Clumps in Saturn's F ring**

*C. D. Murray, N. Cooper, G. A. Williams, M. W. Evans and T. Wong*

Analysis of Cassini ISS observations of Saturn's unusual F ring has already shown that a series of prominent jets (and subsequent strands) observed in late 2006 and early 2007 appears to be associated with collisions between the object S/2004 S 6 and the ring's core (Murray et al., 2008). There is also evidence that the conjunction of a ring segment with Prometheus can trigger the formation of long-lived clumps in the core and that some of these have sufficient mass to perturb surrounding ring material (Beurle et al., 2010). Here we report on a more detailed analysis of F ring strands and clumps. As well as tracking clumps that orbit in or close to the core, we have studied clumps in a bright strand that is likely to have formed in 2007. Objects in the strand are easier to track than those in the core due to the relatively pristine nature of the strand. These clumps have a clear association with Prometheus and may survive for more than one synodic period. We develop simple dynamical models to explain the varying appearance of strands and the orbital evolution of the clumps.

### **The Structures of the Saturnian F ring: Observations and Modeling**

*N. Albers, M. Sremčević, and L.W. Esposito*

The Cassini UVIS instrument has recorded more than 100 stellar occultations of the F ring, Saturn's most dynamic ring, with spatial resolutions ranging between a few and a few tens of meters and various observation geometries. The F ring's main components are core and strands, which are both clearly resolved in the data, allowing for precise measurements of each components location at observation time. Statistically significant small-scale events testify to the evidence of the temporary clumps within the core. Moreover, occultation supporting images for the first time show direct evidence of objects embedded in the F ring core. Here, the camera's pointing was fixed upon a star while the rings are passing through the field of view. This mode of observation provides a method to directly search for objects that are otherwise shrouded in a narrow ring.

We present orbital models for both F ring core and strands that describe the kinematic evolution of these components. On the one hand, the optically thick F ring core is well-described by an inclined, freely precessing ellipse. Signatures of the strong perturbations by the shepherd moon Prometheus can be found in both orbital residuals and peak optical depths. On the other hand, the optically thin strands are transient structures that form the apparent pattern of a kinematic spiral. Our orbital model of the strands consists of a precessing ellipse for each particle of the strand, while their orbital parameters are simple continuous functions of the distance to the F ring core. With only 10 free parameters we successfully fit the observed data and reproduce the expected spiral appearance of the strands in the panoramic mode of observations employed by the imaging team.

## Friday Morning

---

### **The Brightening of Saturn's F Ring**

*Robert S. French, Mark R. Showalter, Rafael Sfair, Carlos Argelles, Myriam Pajuelo, Patricio Becerra, Matthew M. Hedman, and Philip D. Nicholson*

We find that the F ring during the Cassini tour is nearly twice as bright, is three times as wide, and has a higher equivalent depth compared to the ring during the Voyager missions. We have performed photometric measurements of more than 4,800 images of Saturn's F ring taken over a five year period with Cassini's Narrow Angle Camera. We show that a simple model of the ring that uses geometric projection to compensate for viewing angle is inadequate to account for variations in the data, and we have developed a new model based on single-scattering in the presence of shadowing and obscuration. We have also investigated a major, bright feature that appeared in late 2006 and dissipated over the next several years. We have simultaneously determined the increase in brightness due to the new feature (37%), its half-life (331 days), and the mean optical depth ( $\tau \sim 0.044$ ) of the F ring. A similar analysis performed on the images from Voyager 1 and Voyager 2 used by Showalter et al. (1992, Icarus 100, 394), resulted in a lower optical depth ( $\tau \sim 0.026$ ). We further use the Cassini images to measure the mean width of the F ring and use stellar occultations from Voyager PPS and Cassini VIMS to validate both the optical depth and width measurements. In contrast to this decades-scale change, the F ring has not changed significantly during the five years of Cassini observations.

### **The Mass of Transient Clumps in Saturn's F ring**

*Bonnie Meinke, Larry Esposito, Miodrag Sremcevic*

The Cassini Ultraviolet Imaging Spectrograph has detected 27 statistically significant features in 101 occultations by Saturn's F ring since July 2004. Of those 27 features, 17 likely correspond to transient clumps of material. We calculate from these observations the total number and total mass of transient clumps in the F ring. Constraints from observations place an upper limit on the number and total mass of such clumps. In turn, an upper limit on mass means clumps are not spherical, solid objects, rather they are loosely-packed, triaxial ellipsoids elongated in azimuth and vertically flattened. The total mass of clumps in the F ring is thus  $6.1 \times 10^{14}$  kg, the equivalent of a 6.8 km icy moon with a density equivalent to that of Prometheus.

### **The Height of Saturn's F Ring in VIMS and ISS Observations of a Cassini Ring-Plane Crossing**

*Britt R. Scharringhausen, Michael S. Crumrine, Samuel B. Storck-Post, Morgan E. Rehnberg, Sara A. Sans, Samantha M. Wolfe*

In Visual and Infrared Mapping Spectrometer (VIMS) data taken during the ring-plane crossing by the Cassini Spacecraft on 1-2 December 2005, the F ring is vertically unresolved in 150 VIMS QUBs of the sunward ansa of the ring. The QUBs were taken at intervals of less than 10 minutes as Cassini's ring-opening angle decreased from 0.016 to -0.014 degrees. The solar ring-opening angle was -19.5 degrees. Several large clumps orbit through the imaged F-ring ansa. The clumps were removed to create "clean" profiles of vertically-integrated I/F. We present a photometric model of the main rings and (clumpless) F ring. We have varied the vertical profiles of F ring optical depth in the model, and compare the results to the sequence of clean VIF profiles observed at wavelengths of 0.88 and 0.90 microns, in a methane absorption band, chosen so that the disk of the planet is dark and saturnshine is less important. In images from the Narrow Angle Camera of the Imaging Science Subsystem (ISS), the pixel size is 10 km on the ring and the F ring is resolved separately from the main rings, though the F ring's vertical structure is not well-resolved. These clear-filter images are less useful for photometry than the VIMS images, but we use them to place an upper limit on the height of the F ring.

## Friday Morning

---

### **Saturn's F Ring Grains: Aggregates Made of Crystalline Water Ice**

*Sanaz Vahidinia, Jeffrey N. Cuzzi, Matt Hedman, Bruce Draine, Roger N. Clark, Ted Roush, Gianrico Filacchione, Philip D. Nicholson, Robert H. Brown, Bonnie Buratti, and Christophe Sotin*

We present models of the near-infrared ( $1 - 5\mu\text{m}$ ) spectra of Saturn's F ring obtained by Cassini's Visual and Infrared Mapping Spectrometer (VIMS) at ultra-high phase angles ( $177.4 - 178.5^\circ$ ). Modeling this spectrum constrains the size distribution, composition, and structure of F ring particles in the  $0.1-100\ \mu\text{m}$  size range. These spectra are very different from those obtained at lower phase angles; they lack the familiar  $1.5$  and  $2\ \mu\text{m}$  absorption bands, and the expected  $3\ \mu\text{m}$  water ice primary absorption appears as an unusually narrow dip at a shorter wavelength. We have modeled these data using multiple approaches. First, we use a simple Mie scattering model to constrain the size distribution and composition of the particles. The Mie model allows us to understand the overall shapes of the spectra in terms of dominance by diffraction at these ultra-high phase angles, and also to demonstrate that the  $2.86\mu\text{m}$  dip is associated with the Christiansen frequency of water ice (where the real refractive index passes unity). Second, we then use a combination of Mie scattering with Effective Medium Theory to probe the effect of porous (but structureless) particles on the overall shape of the spectrum and depth of the  $2.86\mu\text{m}$  band. Such simple models are not able to capture the shape of this absorption feature well. Finally, we model each particle as an aggregate of discrete monomers, using the Discrete Dipole Approximation (DDA) model, and find a better fit for the depth of the  $2.86\mu\text{m}$  feature. The DDA models imply a slight but noticeable change in the overall size distribution. We present a simple heuristic model which explains the differences between the Mie and DDA model results. We conclude that the F ring contains aggregate particles with a size distribution that is distinctly narrower than a typical power law, and that the particles are predominantly crystalline water ice. Most of the discrepancies between data and theories are in strong resonance-Christiansen frequency regions which are, of course, the most important spectral regions to gaining more insight into these optical regimes

### **Is the F Ring a Dusty Plasma?**

*Frank Crary*

The charging of dust particles by photoelectron currents and the background plasma may significantly influence the dynamics of these particles. This is especially true of sub-micron particles, such as those which may be common in many parts of Saturn's F ring. Based on Cassini/CAPS and RPWS measurements during SOI, ring particle surfaces are likely to charge to a potential of a few volts, and this (depending on the inter-grain distance) account for a large fraction of the negative charge density in the region. This alone may be dynamically significant. However, other collective effects may also become important if these particles are formally a "dusty plasma". This occurs when the inter-grain spacing is of order or smaller than the plasma Debye length, and when the inter-grain electric potential is comparable to the dynamic temperature (relative kinetic energy) of the particles. These collective effects are similar those of self-gravity, common in the dynamics of dense rings. The electromagnetic force between few volt, sub-micron particles is many orders of magnitude greater than the gravitational force between them. Therefore the collective effects of a dusty plasma are significant to orders of magnitude less dense rings than is the case for self-gravity. The observed plasma conditions will be presented and used to determine if the F ring is a dusty plasma (or which parts of the F ring are dusty plasmas) and whether electromagnetic, collective effects are significant.

## Friday Afternoon

---

### Origin of Saturn's Rings via Tidal Stripping from a Lost Titan-Sized Satellite

*R. M. Canup*

Saturn's main rings are  $> 90\%$  water ice by mass. Because bombardment of the rings increases their rock content over time, the rings' current composition implies that they were essentially pure ice when they formed, a much different composition than the roughly half-rock, half-ice mixture expected for a solar abundance of solids. I will here discuss a new ring origin scenario (Canup 2010). Canup & Ward (2006) proposed that Saturn has only one large satellite because large satellites interior to Titan spiraled into Saturn due to density wave interactions with the gaseous protosatellite disk (Type I migration) at the end of the satellite formation era. As a large, Titan-sized satellite approached Saturn, it would likely be differentiated due to the combination of the energy of its formation and strong tidal heating. Planetary tidal forces then preferentially strip mass from the satellite's outer layers prior to its collision with Saturn, leading ultimately to the production of a pure ice ring. The initial ring mass depends on the state of the planet at the time, but can be as large as  $\sim 10^{25}$  g. In its first  $10^8$  yr, the ring's mass decreases to  $\sim \text{few} \times 10^{23}$  g as it viscously spreads. Ring material spreading beyond the Roche limit would accrete into icy moons several hundreds of kilometers in radius, whose orbits would first expand due to resonant torques from the ring and later due to tidal interaction with Saturn. Mimas, Enceladus, and Tethys as a group currently contain  $\sim 90\%$  ice by mass. In the new model, these mid-sized moons (or their progenitors) would have originated from the early primordial ring. This implies a different mode of origin for these inner satellites, which prior works have assumed formed independently of the rings.

### Satellite Formation in the Aftermath of the of Saturn's Rings Formation :

#### A Quantitative Overview

*S. Charnoz, V. Lainey, A. Crida*

The origin of Saturn's mid-sized moons (Mimas, Enceladus, Tethys, Dione and Rhea) is debated: their cratering records show much fewer impacts when scaled to Iapetus, their silicate mass-fraction varies from 6% to 60% and they may have central density concentrations challenging formation models. Recently, some work (Canup, 2010) suggested they could have formed inside the rings, similarly to the smallest moons (Charnoz et al., 2010), but the process was not described nor quantified. Using an hybrid numerical model, we show that accretion within the icy rings can form all mid-sized moons up to Rhea and implant them close to their present location after 2.5 to 4.5 Gyr evolution provided that intense Saturn's tides (Lainey et al., 2010) are considered. Tidal heating related to post-accretional high-eccentricity episodes may explain the signs of geologic activity. Massive irregular chunks of silicates initially present in the rings would be today inside the satellites' core after having accreted an icy shell while being tidally expelled from the rings. This may give birth to moderate-size moons younger than the Solar System, either fully made of ice or differentiated, without the need of radiogenic heating, and with potentially irregular cores as they could be debris from Saturn's rings formation.

## Friday Afternoon

---

### **The Origin of Saturn's Rings**

*I. Mosqueira and P. R. Estrada*

The origin of the majestic rings of Saturn is likely to be intimately connected to that of the Saturnian moons. Yet, the nature of this link remains to be clarified. There are two self-consistent models of regular satellite formation in gaseous and dusty disks (see Estrada et al. 2009). Quite generally, the presence of gas affords opportunities for satellite migration. Indeed, migration leaves no size unaffected from the decoupling size to full-sized satellites. If a large differentiated object migrates within the Roche-limit its icy mantle may be tidally-stripped (e.g., Canup 2010). However, it is quite improbable that such an occurrence can be directly tied to the rings we observe today (Mosqueira and Estrada 2011). Rather, we argue that this process should be seen as one of several that can enrich the ice content of the inner Saturnian disk, including selective gas drag loss of silicates in a cooling subnebula and ablation of a heterogeneous population of interlopers. Given the challenge inherent in retaining a putative primordial icy ring formed in the presence of gas, and the expected subsequent contamination both from subnebula and solar nebula material, it is natural to instead place the origin of the rings at the time of the LHB. In particular, we will discuss a scenario in which a collection of icy moons are subjected to the LHB, generating a debris disk which, once formed, may episodically sustain itself through further free-bound interactions (Estrada and Mosqueira 2006), viscously evolve and spread into the Roche-limit driving pre-existing or re-accreted moons in the process, and leaving behind icy rings as the bombardment tapers off. We will discuss whether this scenario is less restrictive than has been thought (Charnoz et al. 2009).

### **Viscous Spreading of Dense Planetary Rings**

*J. Salmon*

Viscous spreading is a major evolutionary process for all astrophysical disks, and in particular planetary rings, as it globally redistributes the disk's mass and angular momentum. It is also responsible for the disk's losing mass by infall onto the planet, and for bringing material through the Roche limit where accretion becomes possible. The understanding of this process is highly dependent on the model used for the viscosity and thus to the physics responsible for angular momentum transport in the disk. Recent N-body simulations have produced very accurate models for the viscosity of a particulate disk such as Saturn's rings, taking into account the collisions between particles but also the effects of the disk's self-gravity.

Using a 1D hydrocode, I will show that, using the viscosity model of Daisaka et al. (2001), an initially self-gravitating narrow ring undergoes two successive evolutionary stages: (1) a transient rapid spreading while the disk is self-gravitating, with the formation of a density peak inward and an outer region marginally gravitationally stable, and with an emptying time-scale proportional to  $1/M^2$  ( $M$  is the disk's initial mass), and (2) an asymptotic regime where the spreading rate continuously slows down as larger parts of the disk become non-self-gravitating due to the decrease of the surface density, until the disk becomes completely non-self-gravitating. At this point its evolution dramatically slows down, with an emptying time-scale proportional to  $1/M$ , which significantly increases the disk's lifetime compared to previous estimates using constant viscosity. Also, the disk's width scales like  $t^{1/4}$  with the realistic viscosity model, while it scales like  $t^{1/2}$  in the case of constant viscosity, resulting in much larger evolutionary time-scales. I will then discuss implications for the formation and the age of Saturn's rings.

## Friday Afternoon

---

### **The Rate of Impacts on Saturn's Rings**

*Luke Dones, Edward B. Bierhaus, Jr., Jose Luis Alvarelos, Kevin J. Zahnle*

The rate at which bodies, ranging in size from dust grains to Centaurs like Chiron, have traversed the region of Saturn's rings throughout Solar System history determines the degree to which the rings are polluted and the viability of some ring origin scenarios. Prior to Cassini, model impact rates at Saturn were based on the measured size-frequency distribution (SFD) of Jupiter-family comets and the statistics of cometary close encounters with Jupiter, including the Shoemaker-Levy 9 impact (Zahnle et al. 2003). Observations of several impact scars on Jupiter, evidence for collisions of cometary dust grains with the jovian (Showalter et al., 2011) and saturnian rings (Hedman et al., 2011), and measurements of the SFD of craters on young terrains on saturnian moons (e.g., Dones et al., 2009; Bierhaus et al., 2011) provide more direct measurements of the recent flux of km-sized bodies. Modeling the orbital evolution of satellite impact ejecta (Dobrovolskis and Lissauer, 2004; Alvarelos et al. 2005; Bottke et al. 2010) allows estimates of the rings' contamination from within the saturnian system. Finally, the New Horizons Student Dust Counter has measured the flux of micron-sized grains out to Saturn's distance from the Sun and beyond (Poppe et al., 2010). We will discuss how these new developments shed light on the origin and evolution of the rings.

Alvarelos, J.L., et al. 2005. *Icarus* 178, 104.

Bierhaus, E.B., arXiv:1105.2601.

Bottke, W.F., et al., 2010. *Astron. J.* 139, 994.

Dobrovolskis, A.R., Lissauer, J.J. 2004. *Icarus* 169, 462.

Dones, L., et al., 2009. In *Saturn from Cassini-Huygens*, p. 613.

Hedman, M.M. 2011. *Science* 332, 708.

Poppe, A., et al., 2010. *Geophys. Res. Lett.* 37, L11101.

Showalter, M.R. 2011. *Science* 332, 711.

Zahnle, K., et al., 2003. *Icarus* 163, 263.

### **Modeling the Long Term Evolution of the C ring Due to Ballistic Transport**

*P. R. Estrada, R. H. Durisen*

The recent revisiting of the view that the rings may be primordial (and thus originally more massive than is observed today) carries with it the implication that the C ring we currently see could not have been its original incarnation. A calculation of the erosion rate and angular momentum loss of material due to micrometeoroid bombardment and ballistic transport that employs reasonable estimates for the micrometeoroid flux and impact yield would suggest that the C ring is on the order of  $\sim 10^7 - 10^8$  years old. Such an age is further corroborated by "pollution transport" models for the rings in which the exchange of intrinsic and extrinsic material between ring regions darkens the rings to their current state on a similar timescale - an age much younger than would be the case if the rings originated at the time of the LHB, or earlier. If the rings are indeed more massive than previously thought, then the structure we see in the C ring is as a result of processes with timescales shorter than the C ring's lifetime. We model the evolution of the C ring in detail using a combined structural and compositional ballistic transport code we have recently developed. We find, for instance, that plateaus "migrate" inward due to mass and angular momentum transport, and that features in general evolve because different parts of the rings are evolving at different rates due to underlying structure. We also predict that in order for the plateaus to maintain their structure that the viscosity there must be significantly larger than is currently estimated. With our new models, we hope to shed light on the observed C ring structure, most of which remains poorly understood.

## Friday Afternoon

---

### **The Ballistic Transport Instability Revisited**

*Henrik Latter (with Gordon Ogilvie, Marie Chupeau)*

We take a fresh look at the dynamics of the ballistic transport instability, as first proposed by Durisen (1995), and consider its role in the formation of radial wavetrains in the inner B-ring and, possibly, plateaus in the C-ring. The physical problem is reformulated so as to apply to a local patch of disk (the shearing sheet), which, with a few other weak assumptions, considerably simplifies the mathematics. The new streamlined model helps facilitate our physical understanding of the instability, and also makes more tractable the analysis of its nonlinear dynamics. In particular, the formation and characteristics of steady nonlinear wavetrains emerge transparently from the formalism. We present initial results on these nonlinear wavetrains, and their close dependence on the background optical depth (and other parameters).

### **Observations of ejecta clouds produced by impacts onto Saturn's rings**

*Matthew S. Tiscareno, C. J. Mitchell, C. D. Murray, D. DiNino, J. A. Burns, M. M. Hedman, K. Beurle, M. W. Evans, and C. C. Porco*

Quantifying the mass flux onto Saturn's rings has long been a desired goal for several reasons. Mass infall likely dominates the rings' coloration and their levels of non-ice pollution, as well as influencing angular momentum transport and erosion of particles, all of which in turn have the potential to set limits on the age of the rings. Additionally, direct measurement of the mass infall onto Saturn's rings would constrain the population of interplanetary dust in the outer solar system, which is poorly determined at present. However, previous efforts to detect impacts onto Saturn's rings have been unsuccessful.

The first unambiguous images of dust clouds above Saturn's rings, which we interpret as impact clouds, were acquired by the Cassini orbiter during the 2009 saturnian equinox. The main rings provided an unusually dark background, due to sunlight shining edge-on to the dense disk, while dust extending vertically out of the ring plane was fully illuminated. The dust clouds showed evidence of significant keplerian shear, indicating that they were produced within a short period of time and that subsequently each constituent particle evolved on an independent keplerian orbit. One sheared dust cloud was imaged in the C ring ( $\sim 81,600$  km from Saturn center) and a larger one in the A ring ( $\sim 129,400$  km from Saturn center), the latter extending  $\sim 200$  km radially and more than  $5,000$  km azimuthally. The time elapsed since impact (or "age") is indicated by the angle of the sheared structure; the A ring impact was observed on two occasions separated by about a day, and indeed the age of the sheared impact cloud was about 24 hours at the first apparition, and 48 hours at the second.

Several impacts onto Saturn's rings were also likely imaged by Cassini in 2005 in the C ring ( $84,000$  km from Saturn center), enabled by the highest phase angles of any high-resolution image ever obtained of the rings. These structures are smaller and more frequent (they appear in most images with the required phase and resolution) than the 2009 equinox detections, and are smeared by motion of the object during image exposure.

We identify these observed dust clouds as ejecta produced by impacts onto the rings, as this is by far the most likely mechanism for producing such a cloud with the required rapidity. The implications for projectile size, velocity, and frequency will be discussed.

## Friday Afternoon

---

### A Post-Equinox View of Saturn's Rings

*LW Esposito*

Saturn's equinox in August 2009 provided Cassini a spectacular opportunity to observe vertical structure and embedded bodies in Saturn's rings.

This included images of

1. Small bodies in the F ring and outer B ring
2. Vertical excursions at ring edges and other locations

At the same time, occultations show

3. Multimodal structure in the location of the B ring edge and of the CD ringlets
4. F ring features that are likely temporary aggregates and possible small moonlets
5. Small, transparent gaps in the rings, meters to hundreds of meters wide
6. Power spectra indicating objects of scale 200-2000m at the B ring edge and in the strongest density waves

waves

Naturally, the rings appear even more dynamic! In their level of complexity, they resemble a geophysical, more than an astrophysical system. The more detailed rings show the failings of a fluid model: N-body calculations including the relevant physics are necessary, but so slow, they do not help for long-term ring evolution.

Random phenomena are important: comets strike the rings, impacts destroy small moons, embedded and propeller objects represent singular events. What is the balance between deterministic and stochastic forcing? Are the rings near equilibrium or not? Or perhaps cycling?

The ringmoon ellipsoidal shapes, propellers and equinox objects show accretion continues today. If moons aggregate in the Roche zone, they can be driven away by resonance torques and later destroyed to produce new rings (see papers by Charnoz and by Canup).

I favor an ancient, stochastic ring system where individual objects in the rings dominate their immediate vicinity and local evolution. Resonance forcing and Kepler shear provide the energy for a multitude of dynamic phenomena. Ring particles aggregate at perturbed locations, and provide seeds for transient clumps, some of which persist.

I will query the workshop attendees about strengths, weaknesses and tests of this post-Equinox view.

## Practical Matters

---

### Network Connections

Cornell's free network is **RedRover**. Instructions for connecting can be found here:

<http://www.cit.cornell.edu/services/redrover/howto/rrguest/>.

The instructions presented below are for Macintosh OS X (for Windows the procedure is similar):

1. Disconnect any wired (Ethernet or modem) connections.
2. Click the Airport icon on the toolbar, and then click RedRover.  
(In Windows Systems, Connect to RedRover using the appropriate menus)
3. Open any web browser (Firefox, Safari, etc.) to connect to the Internet. A window opens with directions to register for RedRover.
4. In the Registration window, click **Visitors without NetID, Click here to proceed**.
5. The **RedRover Terms of Use** window appears. Read the terms of use and then click **I accept the Above Terms and Conditions**.
6. The Network Registration for Visitors window appears. Fill out the form:
  - In the **E-Mail** box, enter a current e-mail address. You'll receive a confirmation e-mail at this address, so it should be one you can access during your visit to Cornell.
  - In the **Name** box, enter your name.
  - In the **Cornell College or Unit** list, you can accept the default, Unknown.
  - The **Start Date of Visit** displays the current date.
  - In the **Length of Visit** list, select the length of your stay. The maximum registration for guests on RedRover is 21 days.
  - In the **Purpose of Visit** box, enter a brief description of your visit.
7. **Click Register**. You're now registered to use RedRover.
8. Restart your computer, and then you can use the Internet.
9. You'll receive a confirmation message at the e-mail address you entered. Follow the instructions in the message to confirm your registration. (You need to confirm **before midnight** the same day you registered.)

### Lunch Options

Goldie's is located within the Physical Sciences Building. In addition, there are a number of eateries around campus. A map with links can be found here:

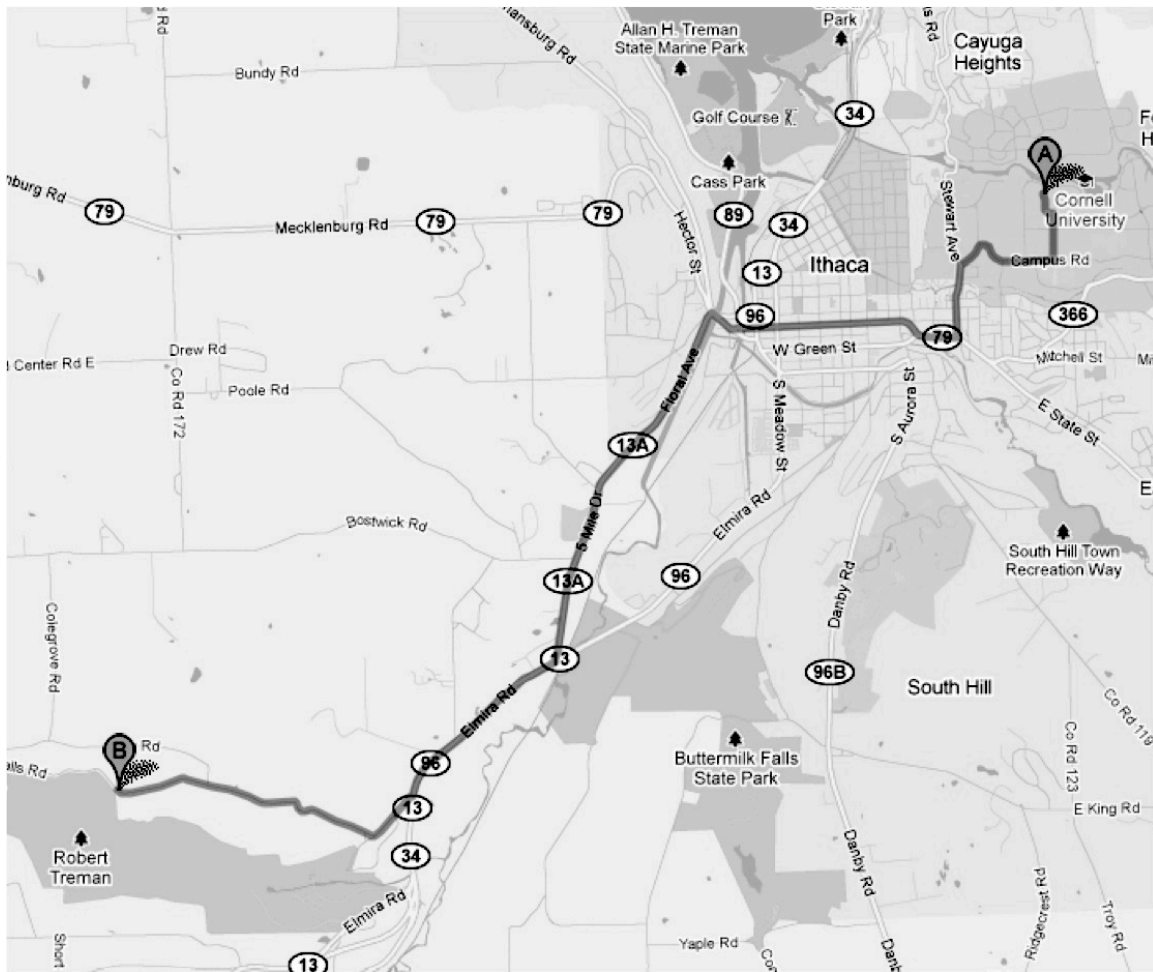
<http://www.campuslife.cornell.edu/campuslife/housing-dining-map.cfm>

If you like, you can place orders in advance via the web by following the instructions here:

<https://cornell.webfood.com/>

Further restaurants can be found in Collegetown, just follow College Avenue south of campus.

## Map to Upper Treman Park (Thursday Picnic Location)



- Get on Route 13A heading south of town
- Continue on Route 13 after it merges with Route 96
- Turn Right onto NY-327 N/Enfield Falls Road
- Drive past the “Lower Park Entrance” for about a mile to the “Upper Park Entrance”.

# Map of Upper Treman Park (Thursday Picnic Location)

